„Dunărea de Jos" University of Galați

Doctoral School for Mechanical and Industrial Engineering

UNIVERSITAS
GALATIENSIS

DOCTORAL THESIS

ABSTRACT

METHODS FOR STUDY OF RECIPROCALLY ENWRAPPING SURFACES WITH APPLICATIONS IN REVERSE ENGINEERING

PhD Student,

Eng. Georgiana-Alexandra COSTIN (MOROȘANU)

Scientific Coordinator,

Prof. dr. eng. hab. Virgil Gabriel TEODOR

Series I 4: Industrial Engineering No. 85

GALATI

2022

„Dunărea de Jos" University of Galați
Doctoral School for Mechanical and Industrial Engineering

UNIVERSITAS
GALATIENSIS

DOCTORAL THESIS

ABSTRACT

METHODS FOR STUDY OF RECIPROCALLY ENWRAPPING SURFACES WITH APPLICATIONS IN REVERSE ENGINEERING

PhD Student,
Eng. Georgiana-Alexandra COSTIN (MOROȘANU)

President	**Prof. univ. dr. eng. Elena SCUTELNICU** "Dunărea de Jos" University of Galati
Scientific Coordinator	**Prof. univ. dr. ing. hab. Virgil Gabriel TEODOR** "Dunărea de Jos" University of Galati
Official Referent	**Prof. univ. dr. ing. ec. Dumitru NEDELCU** Technical University "Gheorghe Asachi" Iasi
Official Referent	**Prof. univ. dr. ing. Gheorghe OANCEA** Transylvania University of Brasov
Official Referent	**Prof. univ. dr. ing. Gabriel-Radu FRUMUȘANU** "Dunărea de Jos" University of Galati

Series I 4: Industrial Engineering No. 85

GALATI

2022

The series of doctoral theses defended publicly in UDJG starting with October 1, 2013 are:

Field **ENGINEERING SCIENCES**

Series I 1:	**Biotechnologies**
Series I 2:	**Computers and information technology**
Series I 3:	**Electrical engineering**
Series I 4:	**Industrial engineering**
Series I 5:	**Material engineering**
Series I 6:	**Mechanical engineering**
Series I 7:	**Food Engineering**
Series I 8:	**Systems Engineering**
Series I 9:	**Engineering and management in agriculture and rural development**

Field **ECONOMICS**

Series E 1:	**Economy**
Series E 2:	**Management**

Field **HUMANITIES**

Series U 1:	**Philology-English**
Series U 2:	**Philology-Romanian**
Series U 3:	**History**
Series U 4:	**Philology-French**

Domeniul **MATHEMATICS AND NATURE SCIENCES**

Series C:	**Chimistry**

ACKNOWLEDGMENTS

With the completion of my doctoral thesis, I would like to address a few words of thanks to all those who guided my steps throughout the three years of doctoral studies.

First of all, I would like to thank my PhD supervisor, Mr. prof. univ. dr. Eng. hab. Virgil Gabriel TEODOR, both for the patience, confidence, support and permanent guidance offered throughout my doctoral studies, as well as for the suggestions and recommendations full of professionalism offered in the elaboration of the doctoral thesis.

At the same time, I would like to thank all the members of the guidance committee, without whom this doctoral thesis could not have been completed: Mr. prof. univ. dr. eng. Nicolae OANCEA, for the shared knowledge and the recommendations permanently offered in the writing of the doctoral thesis, to Mr. prof. univ. dr. eng. Viorel PĂUNOIU, who offered me the chance to be a member of the project "Smart Manufacturing Technologies for Advanced Production of Parts From Automotive and Aeronautics Industries" - TFI PMAIAA, PN-III-P1-1.2-PCCDI-2017-0446, as a research assistant, after which I gained knowledge in the field of reverse engineering and had the opportunity to work with one of the equipment purchased, namely the scanning equipment, which has been useful to me in writing a chapter of this doctoral thesis and, last but not least, I thank Mr. assoc. dr. eng. Nicușor BAROIU, who guided my steps since my undergraduate studies, who supported me, offered me advice and encouraged me whenever I needed in my doctoral years, as well as for the permanent recommendations full of originality offered during the three years of doctoral studies.

At the same time, I would like to thank the official references: Mrs. Dean of the Faculty of Engineering prof. univ. dr. eng. Elena SCUTELNICU, from "Dunărea de Jos" University of Galați, Faculty of Engineering, who agreed to be the president of the doctoral thesis evaluation commission, Mr. prof. univ. dr. eng. ec. Dumitru NEDELCU, from the "Gheorghe Asachi" Technical University of Iasi, Faculty of Mechanical Engineering and Industrial Management, to Mr. prof. univ. dr. eng. Gheorghe OANCEA, from Transilvania University of Brasov, Faculty of Technological Engineering and Industrial Management and to the director of the Department of Manufacturing Engineering, prof. univ. dr. eng. Gabriel-Radu FRUMUȘANU from "Dunărea de Jos" University of Galati, Faculty of Engineering, who agreed to evaluate the doctoral thesis.

I also thank all the professors from the Faculty of Engineering, Manufacturing Engineering department, for their understanding, help and support offered throughout the three years of doctorate and and not only.

Last but not least, I would like to thank the Doctoral School of Mechanical and Industrial Engineering, both the Director of the Doctoral School of Mechanical and Industrial Engineering Mrs. prof. univ. dr. eng. fiz. Luminiţa MORARU, as well as Mrs. Georgeta CRĂCIUN and Mrs. eng. Luiza-Maria AXINTE, for the permanent guidance offered in carrying out all the procedures for completing the doctoral thesis.

skills of organizing, writing scientific articles and presentations from scientific events and conferences, as well as entrepreneurial skills.

On this occasion, I would like to thank all the professors and colleagues I met through the ANTREPRENORDOC project, who shared their knowledge and from whom I had to learn, both professionally and personally: Mr. prof. univ. dr. fiz. Gabriel MURARIU, Mrs. prof. univ. dr. Nicoleta BĂRBUȚĂ-MIȘU, Mrs. assoc. dr. Oana CENAC, Mr. prof. univ. dr. ec. habil. Florin-Marian BUHOCIU, Mr. prof. univ. dr. ec. Adrian MICU and Mr. prof. univ. dr. Marian BARBU.

With all the love and gratitude I have for them, I finally want to thank the members of my family, consisting of my husband, parents, grandmother, in-laws and brothers-in-law, who were by my side, encouraged me, offered advice and moral support throughout my doctoral studies and which will continue to be with me in everything I can do in the future, on all plans.

Thank you all for everything you have taught me!

Kind regards,
Eng. Georgiana-Alexandra COSTIN (MOROȘANU)

Alexandra.Costin@ugal.ro

Galati, June 2022

CONTENT

CHAPTER 1. STATE OF THE ART REGARDING STUDY METHODS FOR RECIPROCALLY ENWRAPPING SURFACES

The generating of surfaces by enwrapping is a problem of utmost importance in the case of cutting processes. This mode of generating has been a continuing concern of researchers and technologists due to the advantages of this mode of generating. Among these advantages are: high productivity and increased machining accuracy, due to the fact that the profile errors of the tool are greatly reduced on the profile of the generated piece [1,2].

Initially, the issue of generating surfaces by enveloping had a graphical approach, due to the difficulties related to the analytical calculation, often very laborious, necessary to solve such problems.

The geometrical methods used in this regard are: the Camus theorem [3], the method based on the fundamental properties of enwrapping curves [4], the Poncelet method (1827) and the Rouleaux method (1842). Subsequently, based on geometric methods, analytical methods for tool profiling were developed, which generate by enwrapping, in particular, by the rolling method [2,5].

Theodore Olivier (1842) developed two fundamental theorems, which bear his name, for the case of generating enveloping surfaces with linear contact and, respectively, with point contact [2,6].

Subsequently, these theorems are reviewed by the mathematician Gohman (1896), who approaches a method that simplifies the way of analyzing the contact of enwrapping surfaces with linear contact and point contact [2,6].

In 1843, the normal theorem, also known as the Willis theorem, was developed for reciprocally enwrapping profiles associated with rolling centrodes [7].

The Nikolaev method (1950) is also another method specific to the profiling of surfaces, reciprocally enveloping, cylindrical or revolutionary [2].

Complementary methods, such as the minimum distance method (1992), method of substituting circles (1998), the tangent method (2000) and the trajectory method (2002), are methods that use the direct way of expressing the enveloping conditions and treat problems specific to the generating of reciprocally enwrapping surfaces [8].

The development of industrial systems, as well as the increasing use of computer numerical controlled (CNC) machine tools, have allowed the generating of complex shaped surfaces, which use circular or rectilinear generating tools. They describe complex trajectories, involving the development of applications for the study of enveloping surfaces made through graphic design programs, such as CATIA, AutoCAD, SolidEdge etc. [9-27].

1.1. Normals method (Willis theorem)

The "*gearing*" theorem, also known as the "*normals method*" or "*Willis theorem*" (1843) [2,28,29] or sometimes as "*Euler–Savary theorem*" [31], can be stated as follows: "*two profiles associated with rolling centrodes, which transmit rotational movement between two parallel axes, are reciprocally enveloping if, in the process of rolling the centrodes, the contact points of the profiles admit a common normal, which passes through the gearing pole*".

Two enwrapping profiles are considered, Figure 1.1, having the two centrodes C_1 and C_2 tangent at the contact point, P. The centrodes rotate around the axes O_1 and O_2 having the velocities expressed by the parameters ω_1 and ω_2.
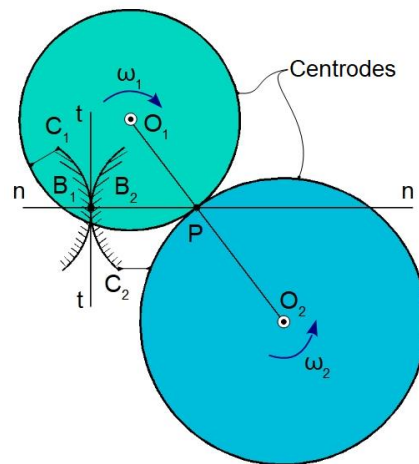
Fig. 1.1. Conjugated profiles [28]

1.2. ”Minimum distance” method

”Minimum distance” method is an analytical method for the study of enwrapping surfaces based on a specific theorem [2,4]: ”*the envelope of a family of plane curves that performs a movement joined with a couple of rolling centrodes is the geometrical locus of the points belonging to the family for which, in the different rolling positions, the distance to the gearing pole is minimal*”, Figure 1.2.
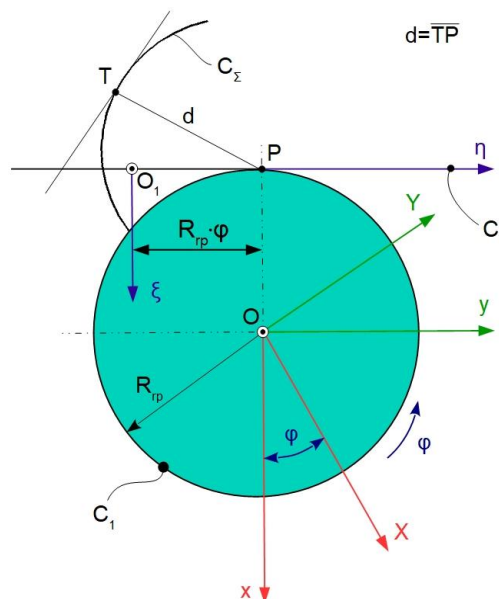
Fig. 1.2. Minimum distance method applied to rack tool generating [4,28]

The following are defined [28]: centrode associated with the vortex of the blank profiles - C_1 (radius circle R_{rp}); entrode associated with the flank of the generating rack - C_2 (line superimposed on the η axis); reference systems: xy - fixed reference system; XY - mobile reference system, joined with the blank; $\xi\eta$ - mobile reference system, joined with the generating rack. The family of profiles, C_Σ, in the $\xi\eta$ system, is described by the transformation:

$$(C_\Sigma)_\varphi = \begin{vmatrix} \xi = X(u) \cdot \cos\varphi - Y(u) \cdot \sin\varphi + R_{rp}; \\ \eta = X(u) \cdot \sin\varphi + Y(u) \cdot \cos\varphi + R_{rp} \cdot \varphi. \end{vmatrix} \qquad (1.1)$$

The minimum condition of distance *d* becomes:

$$\xi \cdot \xi'_u + \left(\eta - R_{rp}\right) \cdot \eta'_u = 0, \tag{1.2}$$

reprezentând „*condiția de înfășurare*" conform acestei metode [28], where ξ'_u and η'_u represent the derivatives of the functions of the rack system *ξη*.

1.3. Trajectory method

Trajectory method is a „complementary method" which is based on determining the enwrapping condition by identifying the trajectories of the points in the tool space, the trajectories tangent to the profile to be generated [4], [28,33]. Figure 1.3 shows a detail of the tool profile and the plane trajectories of the points belonging to the piece`s profile in the tool`s space.
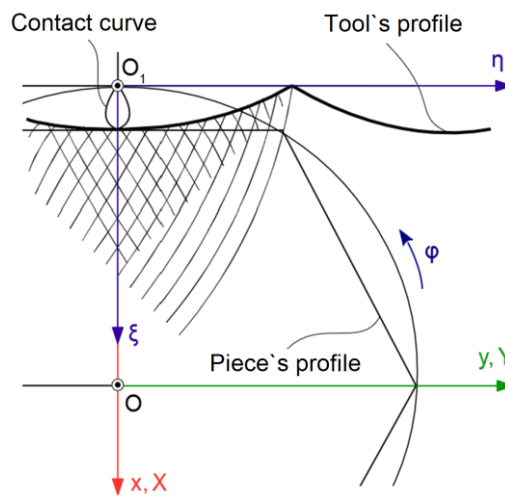
Fig. 1.3. Tool`s profile and the in-plane trajectories of the points belonging to the piece`s profile [4,28]

Metoda traiectoriilor se poate exprima astfel: „*înfășurătoarea unui profil asociat unei centroide, care aparține unui cuplu de centroide în rulare, reprezintă înfășurătoarea traiectoriilor descrise de punctele acestui profil în spațiul asociat centroidei în rulare*" [4], [28].

The parametric equations of the characteristic curve, C_Σ, are [28]:

$$C_\Sigma : \begin{vmatrix} X = X(u); \\ Y = Y(u), \end{vmatrix} \tag{1.3}$$

u being a variable parameter.

The family of trajectories is expressed by the form:

$$(C_\Sigma)_\varphi : \begin{vmatrix} \xi = \xi(u, \varphi); \\ \eta = \eta(u, \varphi). \end{vmatrix} \tag{1.4}$$

Relation (1.4), along with the condition:

$$\frac{\xi'_u}{\xi'_\varphi} = \frac{\eta'_u}{\eta'_\varphi}, \tag{1.5}$$

allows the determination of the profile of the envelope, C_S, which represents the enwrapping curve of the in-plane trajectories of the points belonging to the curve C_Σ, in the rolling movement of the centrode [2,4].

1.4. Profile of tools for generating helical surfaces by kinematic method

The development of graphic design media and computer-aided inspection systems has allowed the development of advanced graphical methods, based on the use of computational techniques and which, in terms of computational accuracy, are equivalent to established analytical methods [26,34]. These methods are mainly used for profiling tools that generate helical surfaces, cases in which analytical methods become difficult to use due to the complexity of the manipulated equations [12,23,25,26,32,35,36,37], [39-44].

One of these methods is the kinematic method, applied to the generation of helical surfaces with disc tools, cylindrical-front tools and cylindrical tools. In the case of disc tools, determining the form of the primary peripheral surface of the tool involves determining the axial section of the rotating surface [2,41]. Thus, being known the helical surface Σ, of $\vec{V}$ axis and parameter p, the rotation surface S can be determined, this being reciprocally enveloping with the Σ surface.

According to Figure 1.4, the reference systems are defined [28]: xyz is a fixed reference system, the z-axis being superimposed on the axis of the rotation surface S; XYZ - mobile reference system, joined with the Σ surface, the Z axis being superimposed on the $\vec{V}$ axis.

In the mobile coordinate system, XYZ, the parametric equations of the helical surface Σ are known:

$$\Sigma: \begin{vmatrix} X = X(u,v); \\ Y = Y(u,v); \\ Z = Z(u,v), \end{vmatrix} \tag{1.6}$$

with u and v independent variables.
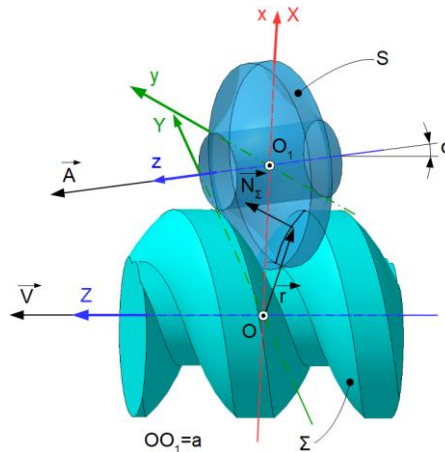
Fig. 1.4. Disc tool-reference systems [28]

The enwrapping condition is:

$$\vec{N}_{\Sigma} \cdot \vec{R}_{\varphi} = 0. \tag{1.7}$$

The axial section of the rotating surface, S, is, in fact, the primary peripheral surface of the tool, which, by means of the equations of the characteristic curve, C, at the fixed coordinate system, xyz, results in the transformation of coordinates:

$$C: \begin{vmatrix} x = X - a; \\ y = Y \cdot \cos\alpha + Z \cdot \sin\alpha; \\ z = -Y \cdot \sin\alpha + Z \cdot \cos\alpha \end{vmatrix} \tag{1.8}$$

The equations of the axial section of the *SA* surface are given by the relation:

$$SA: \begin{vmatrix} R = \sqrt{x^2(u) + y^2(u)}; \\ H = z(u). \end{vmatrix} \tag{1.9}$$

1.5. Helical surfaces generation by decomposing helical movement method - Nikolaev condition

Another complementary method is the Nikolaev condition, also known as the „method of decomposing helical movement" applied to the generation of helical surfaces with disc tools, cylindrical-front tools and cylindrical tools.

In the case of cylindrical-front tools, the helical surface *Σ* is known, this being determined in the helical movement (*V*, *ω*, *p*) of the generating curve, *G* [2,28].

It is required to determine a rotation surface, *S*, with the axis perpendicular to the axis of the *Σ* surface. This surface is obtained from the condition that the *Σ* surface is the envelope of the (*S*) family in the helical movement and admits a common characteristic with the helical surface, *Σ*.

According to Figure 1.5, the following coordinate systems are defined: *xyz* represents the fixed reference system, with the *z* axis superimposed on the surface axis *Σ*; $x_1y_1z_1$ - fixed reference system, the x_1 axis being superimposed on the axis of the sought *S* surface.
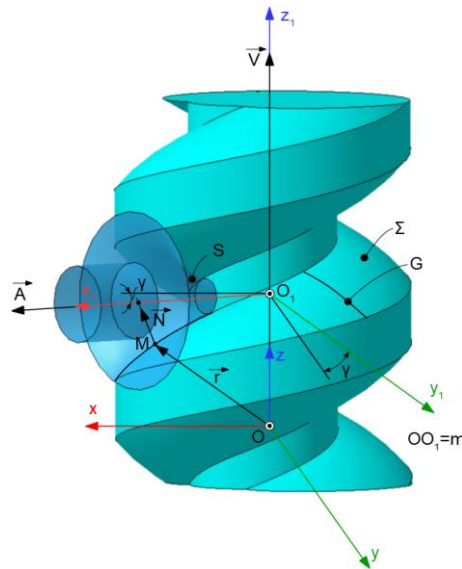
Fig. 1.5. Generating with cylinder-front surface [28]

In the *xyz* coordinate system, the parametric equations of the *Σ* surface are known:

$$\Sigma: \begin{vmatrix} x = x(u,v); \\ y = y(u,v); \\ z = z(u,v). \end{vmatrix} \tag{1.10}$$

The vector of the current point on the *Σ* surface, $\vec{r}$, is determined by the relation:

$$\vec{r} = x(u,v) \cdot \vec{i} + y(u,v) \cdot \vec{j} + z(u,v) \cdot \vec{k}. \tag{1.11}$$

By development, it results the condition for determining the characteristic curve of form:

$$\left[y \cdot N_z - (z - m) \cdot N_y \right] \cdot \cos\gamma - \left[x \cdot N_z - (z - m) \cdot N_x \right] \cdot \sin\gamma = 0. \tag{1.12}$$

Equations (1.10) and (1.12) define the equations of the characteristic curve *C*, common to the surfaces *S* and *Σ*.

If a connection is established between the parameters u and v, of form $u=u(v)$, then the equations of the characteristic curve will be:

$$C: \begin{vmatrix} x = x(v), \\ y = y(v), \\ z = z(v). \end{vmatrix} \tag{1.13}$$

Thus, the parametric equations of the characteristic curve will be brought, in principle, to the form:

$$C: \begin{vmatrix} x_1 = x_1(v), \\ y_1 = y_1(v), \\ z_1 = z_1(v). \end{vmatrix} \tag{1.14}$$

The peripheral surface of the finger cutter tool is obtained by rotating the characteristic curve C around the $\vec{A}$ axis. According to Figure 1.6, the points M and N on the characteristic curve and on the generator are at the same distance from the surface axis x_1.
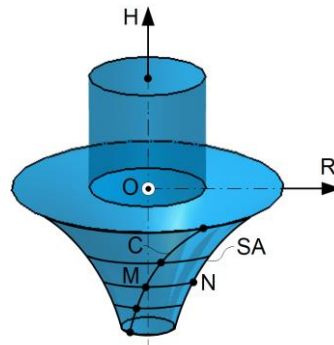
Fig. 1.6. Axial section [28]

Therefore, the parametric equations of the axial section, SA, are given by the relation:

$$SA: \begin{vmatrix} R = \sqrt{y_1^2(v) + z_1^2(v)}; \\ H = x_1(u). \end{vmatrix} \tag{1.15}$$

1.6. Conclusions on the state of the art regarding study methods for reciprocally enveloping surfaces

G The generating of surfaces by enwrapping presupposes the existence of specific methodologies for solving the problem of profiling generating tools. The profiling of tools for generating by enwrapping can be done using the fundamental theorems, applied in the conditions in which the surfaces are considered non-deformable.

These theorems have a high degree of generality and mathematical rigor, but can sometimes be difficult to apply. The way of expressing the enwrapping conditions leads, in many of the practical cases, to laborious analytical calculations and to complicated analytical forms of expression of the equations of the enwrapping surfaces. This led to the development of complementary methods, characterized by a simpler expression of the enwrapping conditions.

Complementary methods are methods that use the direct way of expressing the enwrapping conditions and treat problems specific to the generating of reciprocally enwrapping surfaces. These methods have a simpler form of expression, but a lower degree of generality.

CHAPTER 2. MAIN OBJECTIVES AND RESEARCH DIRECTIONS OF THE DOCTORAL THESIS

Analyzing the methods of profiling the tools that generate by enwrapping by the rolling method, presented in Chapter 1, it can be noticed that the profiling of tools that generate by enveloping by the rolling method, requires the writing of complicated equations, susceptible to errors.

In order to avoid these shortcomings, this doctoral thesis proposes a new method, called the "virtual pole" method, which allows analytical profiling of tools that generate by enwrappinf by the rolling method, avoiding the need to write the equations of relative movements of tool-piece. Using the "virtual pole" method greatly simplifies the calculations required for profiling different types of tools, such as rack tool, gear shaped cutter tool, rotary cutter tool etc., as the determination of the relative movements between the tool and the workpiece and the enwrapping condition are complicated and can be a source of error.

Thus, the main objectives of the doctoral thesis are:
- applying the "virtual pole" theorem to:
    - profiling of rack tools that generate orderly vortices of profiles;
    - generation with gear shaped cutter tools, for ordered vortices of profiles associated with a circular axoid (cylindrical surfaces or helical cylindrical surfaces);
    - generation of non-evolutionary profiles with gear shaped cutter tools (processing of bores with polygonal profiles, inner grooves, square or hexagonal bores or K-profile bores);
    - generation of helical surfaces by enveloping with rotary cutter tools (processing of worm shafts from the composition of gear of worm-worm wheel etc.);
    - profiling of worm tools generating non-evolving teeth (enwrapping surfaces with punctiform contact);
    - profiling the generating tools of the known surfaces in discrete form (actually measured surfaces);
- inspection of reciprocally enwrapping surfaces using a reverse engineering technique;
- study of the enwrapping of the active surfaces of the pieces by analyzing the frontal profiles using the „virtual pole" method.

The research directions resulting from the documentation carried out on the generation of reciprocally enveloping surfaces are:
- realization of numerical applications in specific software products, which allow profiling the types of tools mentioned above, in the main objectives of the doctoral thesis;
- application of three-dimensional measurement techniques, specific to reverse engineering, for the study of enwrapping surfaces, known in discrete form; in order to carry out this process, the parts will be measured by means of existing equipment in the Department of Manufacturing Engineering, within the Faculty of Engineering, "Dunărea de Jos" University of Galați, in order to establish their dimensional characteristics and their modeling will be performed in a computer aided design program;
- performing the inspection in a specific software (GOM Inspect), by overlapping the scanned model and the CAD model of each part, in order to compare the analytical models with the real parts, this comparison allowing the appreciation of the degree to which the analytical model obtained by redesign corresponds to the real piece; in this way, the ability of future parts obtained on the basis of the analytical model to be able to fulfill the desired functional role can be appreciated;

- realization of a study of the enwrapping of the active surfaces of parts of a helical pump by analyzing the frontal profiles using the "virtual pole" method.

Inspecting reciprocally enwrapping surfaces can provide information about the deviations of the parts from the theoretical models.

This provides a solution for limiting scrap and reprocessing parts. This solution involves a pre-measurement of the tools which are going to process the related parts, using the inspection software.

It calculates, based on the measured profile of the tool, which conjugated profile will be obtained for the part and thus there is the possibility to determine if the obtained profile is compliant.

If the calculation shows that the obtained profile, using that cutting tool, shows unacceptable deviations from the nominal profile, the cutting tool will not be used in the manufacturing process or, possibly, will be subjected to a corrective profiling process, which involves changing the tool profile so that the generated profile falls within the permissible tolerance limits.

The innovative character is given by the fact that the software calculates, using the "virtual pole" method, based on the known tool profile, which profile can be obtained for the part.

CHAPTER 3. DEVELOPMENT OF A TOOL PROFILING ALGORITHM THAT GENERATES BY ENWRAPPING - „VIRTUAL POLE" METHOD

In the following, a method is presented to avoid the need to know the relative movement between the two elements involved, namely the piece and the tool.

The new complementary method, called the „virtual pole" method, starts from the premise that, in order to respect the Willis theorem (or the normal method) [2,45], the normal to the profile to be generated, taken by the tangent point to the enveloping profile, must go through the gearing pole. If the normal to the profile Σ (to be generated) carried by a current point of it passes through the gearing pole, it will logically intersect the centrode associated with the Σ profile. Thus, an algorithm can be imagined to determine the intersection point between the normal at profile Σ, taken through the current point and the centrode associated with Σ. This point has been called the "virtual pole". Subsequently, the absolute movement of the tool is applied to this "virtual pole" until its position coincides with the gearing pole.

3.1. Rack tool profiling
3.1.1. Profiling algorithm

Generating with rack tool is a particular case of gearing between profiles that transmit rotation movement, which is characterized by the fact that one of the centrodes radii associated with the two profiles has infinite value [46]. Profiling rack tool involves the use of three reference systems, Figure 3.1 [46]: xOy - fixed system, having the origin in the centre of the rolling circle of the piece; XOY - mobile reference system associated with the generated profile (the rotation angle of this system is notated with φ); $\xi O_1 \eta$ - mobile reference system associated with the tool`s centrode, C_2, joined with the tool. The rolling condition of the two centrodes: C_1 joined with the piece and C_2 joined with the future rack tool is given by the condition:

$$\delta = R_{rp} \cdot \varphi. \tag{3.1}$$

Virtual pole is defined as the intersection point between the normal to the Σ profile, taken through the M point on the profile to be generated and the centrode associated with the piece - radius circle - R_{rp}.

In the rolling process of the two centrodes, with condition: $\delta = R_{rp} \cdot \varphi$, virtual pole P_v will overlap, for a certain value of parameter φ, with the gearing pole P - the tangent point of C_1 and C_2 centrodes.

For a certain value of the parameter u, the position vector of the virtual pole, corresponding to the current point $M(X(u); Y(u))$ has the equation:

$$\vec{r}_{P_v} = \vec{r} + \vec{N}_\Sigma = \left(X(u) \cdot \vec{i} + Y(u) \cdot \vec{j} \right) + \lambda \cdot \left[\dot{Y}_u \cdot \vec{i} - \dot{X}_u \cdot \vec{j} \right] = \left[X(u) + \lambda \cdot \dot{Y}_u \right] \cdot \vec{i} + \left[Y(u) - \lambda \cdot \dot{X}_u \right] \cdot \vec{j}. \tag{3.2}$$

The C_1 centrode (circle of radius R_{rp}) has the parametric equations:

$$C_1 : \begin{vmatrix} X = -R_{rp} \cdot \cos \varphi; \\ Y = R_{rp} \cdot \sin \varphi, \end{vmatrix} \tag{3.3}$$

The enwrapping condition is given by the relation:

$$-\left[R_{rp} \cdot \cos \varphi + X(u) \right] \cdot \dot{X}_u + \left[R_{rp} \cdot \sin \varphi - Y(u) \right] \cdot \dot{Y}_u = 0. \tag{3.4}$$

The gearing curve, Figure 3.2, is given by the relation:

$$x = \omega_3^T \left(\varphi_u \right) \cdot X. \tag{3.5}$$

Development of a tool profiling algorithm that generates by enwrapping -
„virtual pole" method
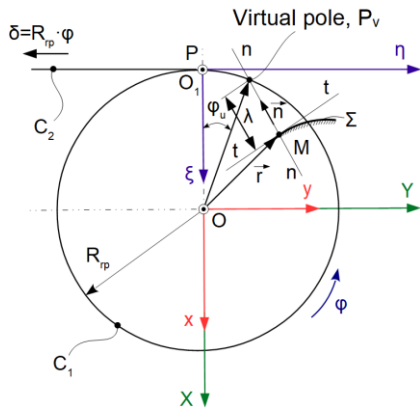
Fig. 3.1. Rolling centrodes, C_1, C_2; reference systems; gearing pole, P and virtual pole, P_v [46]
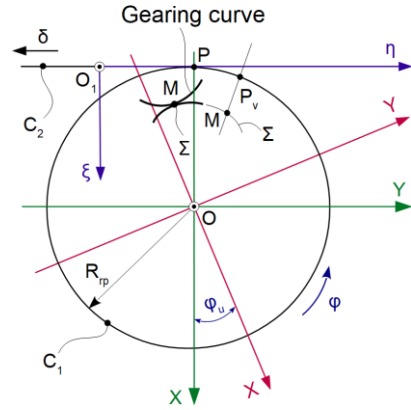
Fig. 3.2. Transposition of the current point, M on the Σ profile on the gearing curve [46]

3.1.2. Application - Rack for a square shaft

The tangent point coordinates between the tool profile and the piece profile will be given by the equations:

$$S: \begin{vmatrix} \xi = -a \cdot cos\,\varphi_u - u \cdot sin\,\varphi_u + R_{rp}; \\ \eta = -a \cdot sin\,\varphi_u + u \cdot cos\,\varphi_u + R_{rp} \cdot \varphi_u; \\ \varphi_u = arcsin\left(\dfrac{u}{R_{rp}}\right). \end{vmatrix} \tag{3.6}$$

The profile of the generating tool was calculated for a shaft-type piece with a square section. The graphical representation of the rack profile is presented in Figure 3.3.
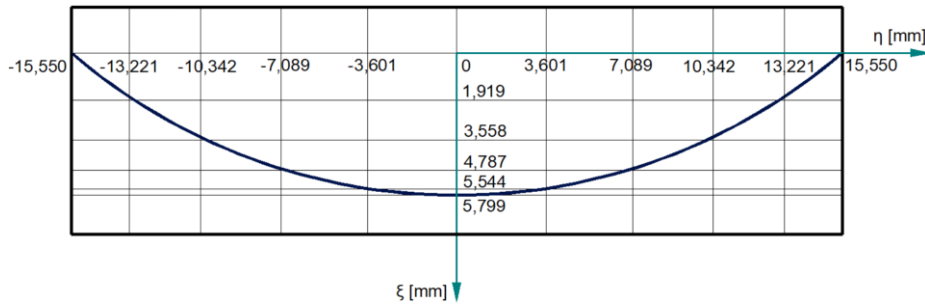
Fig. 3.3. Rack tool profile [46]

It can be observed that the results obtained are identical to those obtained using established methods of profiling of tools that generate by enwrapping, by the rolling method (Gohman theorem or Normals theorem).

3.1.3. Application - Generating rack of the involute flank

Figure 3.4 shows the rack tool for generating an involute flank. The involute profile equations will be [47]:

$$\Sigma: \begin{vmatrix} X(u) = -R_b \cdot cos\,u - R_b \cdot u \cdot sin\,u; \\ Y(u) = R_b \cdot sin\,u - R_b \cdot u \cdot cos\,u. \end{vmatrix} \tag{3.7}$$

The position vector of the virtual pole corresponding to the current point M is given by [47]:

$$\vec{r}_{P_v} = \left(X(u) + \dot{Y}_u \cdot \lambda\right) \cdot \vec{i} + \left(Y(u) - \dot{X}_u \cdot \lambda\right) \cdot \vec{j}, \tag{3.8}$$

where λ is a scalar variable in the direction of normal and *X(u), Y(u)* - the parametric equations of the profile which, for a certain value of u, will give the coordinates of the current point, *M*.
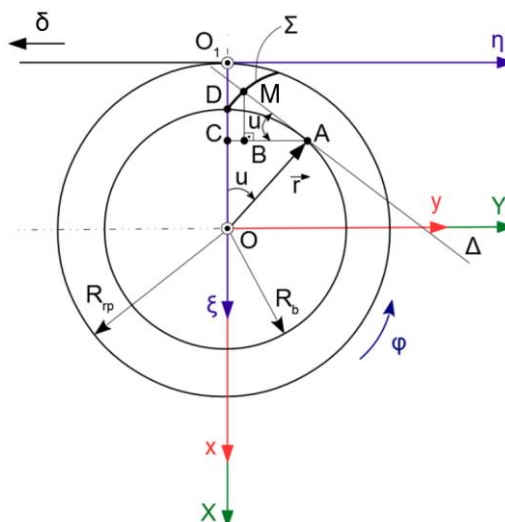
Fig. 3.4. The rack tool for generating an involute flank [47]

The profile of the generating tool is obtained by associating with the tool's movement eequations, the enwrapping condition. Specifically, for a certain value of the parameter *u*, the value of the angle *φ* with which the piece must be rotated is calculated, so that the virtual pole overlaps the gearing pole [47]:

$$\varphi_u = arccos\left(\frac{R_b}{R_{rp}}\right) + u. \tag{3.9}$$

For $u = u_M$, the coordinates of the current point in the fixed reference system will be:

$$M: \begin{vmatrix} x_M = -R_b \cdot cos(u_M - \varphi_u) - R_b \cdot u_M \cdot sin(u_M - \varphi_u); \\ y_M = R_b \cdot sin(u_M - \varphi_u) - R_b \cdot u_M \cdot cos(u_M - \varphi_u). \end{vmatrix} \tag{3.10}$$

Given that the tool is currently displaced according to the φ_u value, the coordinates of the current point in the tool reference system will be [47]:

$$M: \begin{vmatrix} \xi_M = x_M + R_{rp}; \\ \eta_M = y_M + R_{rp} \cdot \varphi_u. \end{vmatrix} \tag{3.11}$$

The profile of the generating tool *S* is calculated, having the following input data: R_b=50 mm, R_{rp}=52 mm, u_{min}=0 rad and u_{max}=0,262 mm. The numerical results are given in the table 3.1.

Table 3.1. Coordinates of the points on the tool profile [47]

Crt. no.	ξ [mm]	η [mm]	Nr. crt.	ξ [mm]	η [mm]
1	3,929	0,709	12	5,761	1,345
2	4,081	0,832	13	5,929	1,396
3	4,249	0,884	14	6,097	1,447
4	4,417	0,935	15	6,265	1,498
5	4,585	0,986	16	6,433	1,550
6	4,753	1,037	17	6,601	1,601
7	4,921	1,089	18	6,769	1,652
8	5,089	1,140	19	6,937	1,703
9	5,257	1,191	20	7,105	1,754
10	5,425	1,242	21	7,273	1,806
11	5,593	1,293			

Development of a tool profiling algorithm that generates by enwrapping -
„virtual pole" method

3.2. Gear shaped cutter tool profiling

In order to determine the tool profile intended to process, by enveloping, by the rolling method, a profile Σ known in analytical or discrete form (by measurement), 3 reference systems are considered, Figure 3.5: *xy* - fixed reference system, with the origin in the center of the rolling circle of the piece; x_0y_0 - fixed reference system, with the origin in the center of the rolling circle of the tool; *XY* - the mobile reference system, joined with the piece; *ξη* - the mobile reference system, joined with the tool. The following notations will be used [45]: C_1 - centrode of the piece; C_2 - centrode of the tool; P_v - virtual pole; *T* - current point; *P* - gearing pole, the tangency point of the rolling centrodes; *Σ* - generated profile; *S* - profile to be generated (reciprocally enveloping with Σ); *CC* - gearing curve.

3.2.1. Profiling algorithm

In the case of the gear shaped cutter tool, the absolute movements of the piece and the tool are rotational movements, Figure 3.5. The rolling condition between the two centrodes, both of circle type, is the condition that they roll without sliding: [45]:

$$R_{rp} \cdot \varphi_1 = R_{rs} \cdot \varphi_2 \Leftrightarrow \varphi_2 = \frac{R_{rp}}{R_{rs}} \cdot \varphi_1 = i \cdot \varphi_1. \tag{3.12}$$

The normal vector at profile *Σ*, having the module *λ*, is given by the equation:

$$\vec{N}_\Sigma = \lambda \cdot \left(\dot{Y}_u \cdot \vec{i} - \dot{X}_u \cdot \vec{j} \right). \tag{3.13}$$

The position vector of the current point *T* is given by:

$$\vec{r} = X(u) \cdot \vec{i} + Y(u) \cdot \vec{j}. \tag{3.14}$$

By summing the two vectors, $\vec{r}$ and $\vec{N}_\Sigma$, the position vector of the virtual pole is obtained, Figure 3.6.
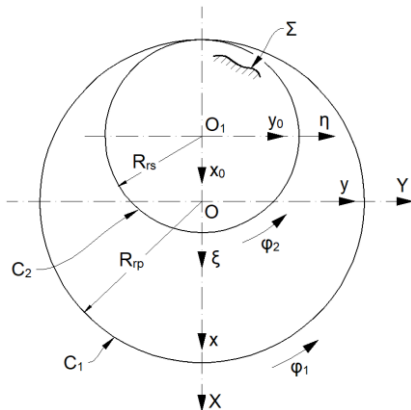
Fig. 3.5. Generating with gear shaped cutter tool. Rolling centrodes and reference systems [45]
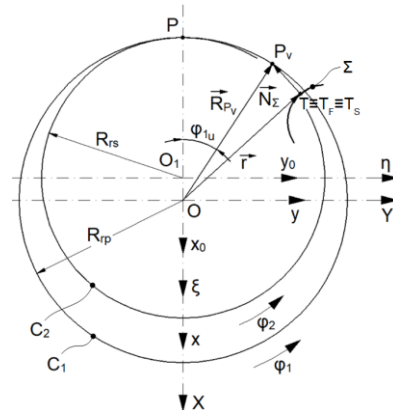
Fig. 3.6. Generating with inner rotary cutter. Rolling centrodes [45]

$$\vec{R}_{P_v} = \vec{r} + \vec{N}_\Sigma = X(u) \cdot \vec{i} + Y(u) \cdot \vec{j} + \lambda \cdot \left(\dot{Y}_u \cdot \vec{i} - \dot{X}_u \cdot \vec{j} \right) =$$
$$= \left[X(u) + \lambda \cdot \dot{Y}_u \right] \cdot \vec{i} + \left[Y(u) - \lambda \cdot \dot{X}_u \right] \cdot \vec{j}. \tag{3.15}$$

Cunoscute fiind ecuațiile parametrice ale centroidei C_1 se poate determina valoarea scalarului *λ*, pentru care este respectată definiția polului P_v [45]:

$$\begin{vmatrix} X = -R_{rp} \cdot \cos \varphi_{1_u} = X(u) + \lambda \cdot \dot{Y}_u; \\ Y = R_{rp} \cdot \sin \varphi_{1_u} = Y(u) - \lambda \cdot \dot{X}_u. \end{vmatrix} \tag{3.16}$$

The parameter λ can be removed from the system of equations (3.16) [45]:

$$\lambda = \frac{-R_{rp} \cdot \cos\varphi_{1_u} - X(u)}{\dot{Y}_u} = \frac{-R_{rp} \cdot \sin\varphi_{1_u} + Y(u)}{\dot{X}_u}. \tag{3.17}$$

From equation (3.17) the enwrapping condition results:

$$\left[-R_{rp} \cdot \cos\varphi_{1_u} - X(u)\right] \cdot \dot{X}_u = \left[-R_{rp} \cdot \sin\varphi_{1_u} + Y(u)\right] \cdot \dot{Y}_u, \tag{3.18}$$

Therefore, for the current value of the parameter u, the value φ_{1u}, given by (3.18) represents the angle at which the blank should be rotated so that the virtual pole occupies the position P.

The point T_F, in the xy system, has the coordinates [45]:

$$T_F: \begin{vmatrix} x = X(u) \cdot \cos\varphi_{1u} - Y(u) \cdot \sin\varphi_{1u}; \\ y = X(u) \cdot \sin\varphi_{1u} + Y(u) \cdot \cos\varphi_{1u}, \end{vmatrix} \tag{3.19}$$

and will belong to the gearing curve.

At this moment, the T and T_F points coincide and, moreover, are on the profile S of the tool. Their coordinates, in the reference system associated with the tool, can be determined by transforming coordinates corresponding to the absolute movement of the tool [45]:

$$\begin{vmatrix} \xi = x_0 \cdot \cos(\pm\varphi_2) - y_0 \cdot \sin(\pm\varphi_2); \\ \eta = x_0 \cdot \sin(\pm\varphi_2) + y_0 \cdot \cos(\pm\varphi_2). \end{vmatrix} \tag{3.20}$$

where "+" is for internal generation and "-" for external generation, representing the transposition of the gearing curve in the tool system, so the profile of the gear shaped cutter tool.

So, the TS point on the tool profile and which coincides with the T_F-point on the gearing curve and with the T-point on the profile Σ will have the coordinates [45]:

$$T_S: \begin{vmatrix} \xi_{T_S} = \left(x_{T_F} + A_{12}\right) \cdot \cos(\pm\varphi_2) - y_{T_F} \cdot \sin(\pm\varphi_2); \\ \eta_{T_S} = \left(x_{T_F} + A_{12}\right) \cdot \sin(\pm\varphi_2) + y_{T_F} \cdot \cos(\pm\varphi_2). \end{vmatrix} \tag{3.21}$$

3.2.2. Application - Gear shaped cutter tool for the generation of a K-type bore

Figure 3.7 shows the reference systems [48]: xy fixed reference system; XY - mobile reference system, in joined with the profile to be generated, Σ; C_1 - centrode associated with the piece.

At the current point T, belonging to the profile Σ, which must be generated, the normal $\vec{N}_\Sigma$ has been taken. It intersects the C_1 centrode at the P_v point, a point representing the virtual pole.

The vector of the normal at this point will take the form:

$$\vec{N}_\Sigma = \lambda \cdot \left(\dot{Y}_u \cdot \vec{i} - \dot{X}_u \cdot \vec{j}\right), \tag{3.22}$$

λ - being a scalar size that represents the distance between the current point T and the virtual pole P_v.

The position vector of the point P_v is obtained by summing the vectors $\vec{r}$ and $\vec{N}_\Sigma$ obtaining the form [45]:

$$\vec{r}_{P_v} = \vec{r} + \vec{N}_\Sigma = \left[X(u) + \lambda \cdot \dot{Y}_u\right] \cdot \vec{i} + \left[Y(u) + \lambda \cdot \dot{X}_u\right] \cdot \vec{j}. \tag{3.23}$$

***Development of a tool profiling algorithm that generates by enwrapping -
„virtual pole" method***
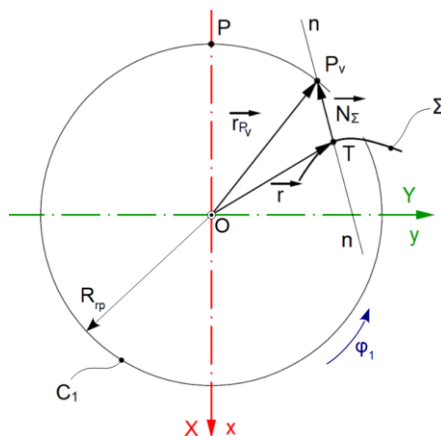
Fig. 3.7. Virtual pole identification [48]

The centrode equations are [48]:

$$C_1: \begin{vmatrix} X = -R_{rp} \cdot cos\,\varphi_1; \\ Y = R_{rp} \cdot sin\,\varphi_1 \end{vmatrix} \qquad (3.24)$$

and thus the belonging condition becomes:

$$\begin{cases} -R_{rp} \cdot cos\,\varphi_1 = X(u) + \lambda \cdot \dot{Y}_u; \\ R_{rp} \cdot sin\,\varphi_1 = Y(u) + \lambda \cdot \dot{X}_u. \end{cases} \qquad (3.25)$$

From the system of equations (3.25) the parameter λ can be removed, obtaining [48]:

$$\left[-R_{rp} \cdot cos\,\varphi_1 - X(u) \right] \cdot \dot{X}_u - \left[R_{rp} \cdot sin\,\varphi_1 - Y(u) \right] \cdot \dot{Y}_u = 0, \qquad (3.26)$$

epresenting the winding condition, meaning the connection between the independent parameters u and φ_1.

Odată cunoscută valoarea specifică $\varphi_1 = \varphi_{1u}$, pentru care punctul P_v coincide cu polul angrenării, poate fi determinată poziția punctului T, în mișcarea sa absolută:

$$x = \omega_3^T \left(\varphi_{1u} \right) \cdot X(u), \qquad (3.27)$$

adică poziția pe care o ocupă acesta pe linia de angrenare, în procesul rulării [48]:

$$T_F \begin{vmatrix} x(u,\varphi_{1u}) = X(u) \cdot cos\,\varphi_{1u} - Y(u) \cdot sin\,\varphi_{1u}; \\ y(u,\varphi_{1u}) = X(u) \cdot sin\,\varphi_{1u} + Y(u) \cdot cos\,\varphi_{1u}. \end{vmatrix} \qquad (3.28)$$

Taking into account the enwrapping condition:

$$R_{rp} \cdot \varphi_1 = R_{rs} \cdot \varphi_2 \Rightarrow \varphi_2 = \left(\frac{R_{rp}}{R_{rs}} \right) \cdot \varphi_1 = i \cdot \varphi_1, \qquad (3.29)$$

the position of the tool can be determined when the part rotates at an angle φ_{1u}, Figure 3.8.

The absolute movement of the tool is [48]:

$$\xi = \omega_3^T \left(\varphi_2 \right) \cdot x_0 = \omega_3^T \left(i \cdot \varphi_1 \right) \cdot x_0. \qquad (3.30)$$
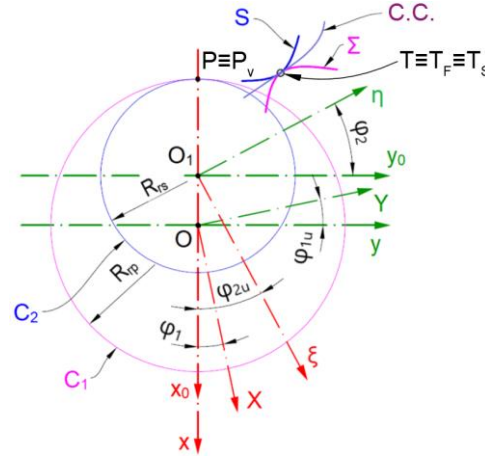
Fig. 3.8. The correlation between the movements of the piece and the tool [48]

Applying to this point the absolute movement of the tool, given by (3.30), its coordinates are obtained in the reference system $\xi\eta$, associated with the tool [48]:

$$T_S: \begin{vmatrix} \xi_{T_S} = x_{T_{F0}} \cdot cos\left(i \cdot \varphi_{1u}\right) - y_{T_{F0}} \cdot sin\left(i \cdot \varphi_{1u}\right); \\ \eta_{T_S} = x_{T_{F0}} \cdot sin\left(i \cdot \varphi_{1u}\right) + y_{T_{F0}} \cdot cos\left(i \cdot \varphi_{1u}\right) \end{vmatrix} \tag{3.31}$$

When the current point T traverses the entire Σ profile, the T_S point traverses the entire profile S, reciprocally enveloping the Σ profile [48]. The equations of the K-type profile are given by:

$$\Sigma: \begin{vmatrix} X(u) = \left[R - e \cdot cos(n \cdot u)\right] \cdot cos\,u - n \cdot e \cdot sin(n \cdot u) \cdot sin\,u; \\ Y(u) = \left[R - e \cdot cos(n \cdot u)\right] \cdot sin\,u + n \cdot e \cdot sin(n \cdot u) \cdot cos\,u, \end{vmatrix} \tag{3.32}$$

where n is the number of lobes and e is the eccentricity.

The movement parameter of this system is the angle φ_2, related to the angle φ_1, by the rolling condition:

$$\varphi_2 = \frac{R_{rp}}{R_{rs}} \cdot \varphi_1 = i \cdot \varphi_1. \tag{3.33}$$

According to the equation (3.22), the normal to the Σ profile at T point is:

$$\vec{N}_\Sigma = \lambda \cdot \left\{ -\left[e \cdot \left(1 - n^2\right) \cdot cos(n \cdot u) - R\right] \cdot cos\,u \cdot \vec{i} - \right.$$
$$\left. -\left[e \cdot \left(1 - n^2\right) \cdot cos(n \cdot u) - R\right] \cdot sin\,u \cdot \vec{j} \right\}. \tag{3.34}$$

The position vector of the T point is given by:

$$\vec{r} = \left\{ \left[R - e \cdot cos(n \cdot u)\right] \cdot cos\,u - n \cdot e \cdot sin(n \cdot u) \cdot sin\,u \right\} \cdot \vec{i} +$$
$$+ \left\{ \left[R - e \cdot cos(n \cdot u)\right] \cdot sin\,u + n \cdot e \cdot cos(n \cdot u) \cdot cos\,u \right\} \cdot \vec{j}. \tag{3.35}$$

As a result, according to (3.23), the position vector of the virtual pole is:

$$\vec{r}_{P_v} = \vec{N}_\Sigma \cdot \vec{r} = \left\{ \left[R - e \cdot cos(n \cdot u)\right] \cdot cos\,u - n \cdot e \cdot sin(n \cdot u) \cdot sin\,u - \right.$$
$$\left. -\lambda \cdot \left[e \cdot \left(1 - n^2\right) \cdot cos(n \cdot u) - R\right] \right\} \cdot cos\,u \cdot \vec{i} +$$
$$+ \left\{ \left[R - e \cdot cos(n \cdot u)\right] \cdot sin\,u + n \cdot e \cdot sin(n \cdot u) \cdot cos\,u - \right.$$
$$\lambda \cdot \left[e \cdot \left(1 - n^2\right) \cdot cos(n \cdot u) - R\right] \cdot sin\,u \right\} \cdot \vec{j}. \tag{3.36}$$

***Development of a tool profiling algorithm that generates by enwrapping -
„virtual pole" method***

The specific form of the enwrapping condition is:

$$\varphi_{1_u} = -u - arcsin\left[\frac{n \cdot e \cdot sin(n \cdot u)}{R_{rp}}\right].$$ (3.37)

For a certain value of the parameter u and a corresponding value φ_{1u}, determined from the enwrapping condition (3.37), the T point, belonging to the Σ profile, will have, in the fixed reference system, the coordinates given by the absolute movement of the blank [48]:

$$T:\left|\begin{matrix}x_{T_F} = X_T \cdot cos\,\varphi_{1u} - Y_T \cdot sin\,\varphi_{1u}; \\ y_{T_F} = X_T \cdot sin\,\varphi_{1u} + Y_T \cdot cos\,\varphi_{1u}.\end{matrix}\right.$$ (3.38)

The position of the tool reference system is given by its absolute movement [48]:

$$T_S:\left|\begin{matrix}\xi = x_0(u) \cdot cos\,\varphi_2 + y_0(u) \cdot sin\,\varphi_2; \\ \eta = -x_0(u) \cdot sin\,\varphi_2 + y_0(u) \cdot cos\,\varphi_2,\end{matrix}\right.$$ (3.39)

So, considering (3.39) it results:

$$T_S:\left|\begin{matrix}\xi_{T_S} = x_{T_{F_0}} \cdot cos\,\varphi_{2u} + y_{T_{F_0}} \cdot sin\,\varphi_{2u}; \\ \eta_{T_S} = x_{T_{F_0}} \cdot sin\,\varphi_{2u} - y_{T_{F_0}} \cdot cos\,\varphi_{2u}.\end{matrix}\right.$$ (3.40)

For a profile defined by *R=60 mm; e=5 mm; n=3 lobes* (according to DIN 32711), the profile to be generated, the gearing curve and the profile of the generating tool are shown in Figure 3.9 [48].
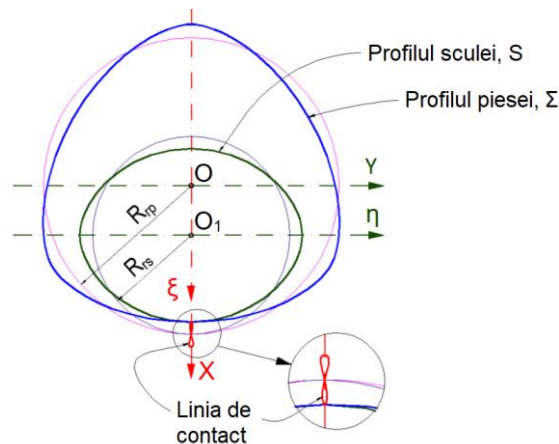
Fig. 3.9. The profile to be generated, the gearing curve and the profile of the generating tool [48]

3.3. Rotary cutter tool profiling
3.3.1. Profiling algorithm

In the case of the rotary cutter tool, the absolute movement of the tool is a rotational movement and the absolute movement of the piece is a translational movement. In this case, the C_1 centrode associated with the piece is a line, while the C_2 centrode, associated with the tool, is a radius circle R_{rp} [45].

The specific form of the enwrapping condition will be:

$$-X(u) \cdot \dot{X}_u = [-\delta + Y(u)] \cdot \dot{Y}_u.$$ (3.41)

The δ_u value represents the translation value of the *XY* system, associated to the piece, which ensures the position of the P_v-point in the gearing pole. For this movement, the current point *T* will have the coordinates given by its absolute movement [45]:

$$T_F:\begin{vmatrix} x_{T_F} = X_T + R_{rs}; \\ y_{T_F} = Y_T - \delta_u. \end{vmatrix}$$

(3.42)

The T_S-point on the tool profile and which coincides with the *T*-point on the profile *Σ* and with the T_F-point on the gearing curve will have the coordinates given by the absolute movement of the tool which is the rotation movement..

Taking into account the rolling condition which can be also written as $\varphi_1 = \dfrac{\delta_u}{R_{rs}}$, is obtained:

$$T_S:\begin{vmatrix} \xi_{T_S} = x_{T_F} \cdot cos\left(\dfrac{\delta_u}{R_{rs}}\right) + y_{T_F} \cdot sin\left(\dfrac{\delta_u}{R_{rs}}\right); \\ \eta_{T_S} = -x_{T_F} \cdot sin\left(\dfrac{\delta_u}{R_{rs}}\right) + y_{T_F} \cdot cos\left(\dfrac{\delta_u}{R_{rs}}\right), \end{vmatrix}$$

(3.43)

representing the transfer of the gearing curve in the *ξη* system meaning the analytical form of the rotary cutter tool.
.

3.3.2. Application - Rotary cutter tool for the processing of a ball screw

The rolling condition has the form:

$$\delta = R_{rs} \cdot \varphi.$$

(3.44)

The normal at *Σ* profile is given by the equation:

$$\vec{N}_\Sigma = \left(-r \cdot cos\,u \cdot \vec{i} - r \cdot sin\,u \cdot \vec{j}\right) \cdot \lambda.$$

(3.45)

In the equation (3.45), *λ* represents the the modulus of a vector with the origin in the current point *T* belonging to the *Σ* profile and the peak on the C_1 centrode, at the P_v point. The point P_v represents the virtual pole [49].

The position vector of the P_v point can be determined by summing the vectors $\vec{r}$ and $\vec{N}_\Sigma$:

$$\vec{r}_{P_v} = \vec{r} + \vec{N}_\Sigma = \left(a - r \cdot cos\,u - r \cdot \lambda \cdot cos\,u\right) \cdot \vec{i} + \left(b - r \cdot sin\,u - r \cdot \lambda \cdot sin\,u\right) \cdot \vec{j}.$$

(3.46)

According to the virtual pole method, for a certain value of the parameter *u*, δ_u can be identified for which, during the absolute movement of the piece, the P_v point coincides with the gearing pole, *P* [49]:

$$\delta_u = \dfrac{b \cdot cos\,u - a \cdot sin\,u}{sin\,u}.$$

(3.47)

The coordinates of the current point *T*, in the fixed reference system, will be [49]:

$$T:\begin{vmatrix} x_T = a - r \cdot cos\,u - R_{rs}; \\ y_T = a + b - r \cdot sin\,u - \dfrac{b \cdot cos\,u}{sin\,u}. \end{vmatrix}$$

(3.48)

When u varies from u_{min} to u_{max}, the point *T* traverses the gearing curve. Therefore, the parametric equations of the gearing curve will be [49]:

$$CA: \left| \begin{array}{l} x(u) = a - r \cdot \cos u - R_{rs}; \\ y(u) = a + b - r \cdot \sin u - \dfrac{b \cdot \cos u}{\sin u}. \end{array} \right. \tag{3.49}$$

For a certain value of u, the coordinates of the T point are:

$$\left| \begin{array}{l} \xi_T = x_T \cdot \cos \varphi_u + y_T \cdot \sin \varphi_u; \\ \eta_T = -x_T \cdot \sin \varphi_u + y_T \cdot \cos \varphi_u. \end{array} \right. \tag{3.50}$$

Therefore, when u takes values from u_{min} to u_{max}, T point will traverse the entire S profile. Thus, a numerical application has been made in the Octave program for profiling the rotary cutter tool, designed to process a ball screw with the axial section shown in Figure 3.10. The dimensions of this profile are: *a=0,17 mm; b=0,155 mm; R_{rs}=50 mm; r=5,4 mm*. Figure 3.11 shows graphically the profile of the generating tool and the contact curve [49].
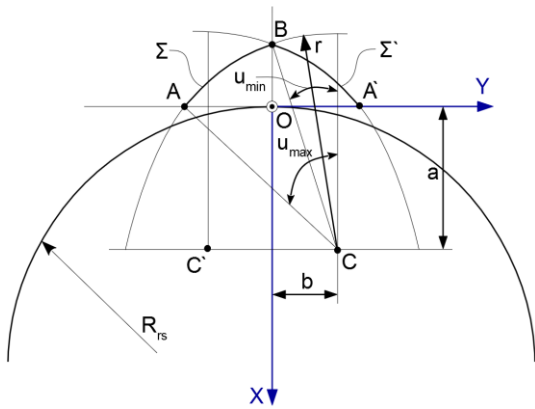
Fig. 3.10. Axial section of the ball screw [49]
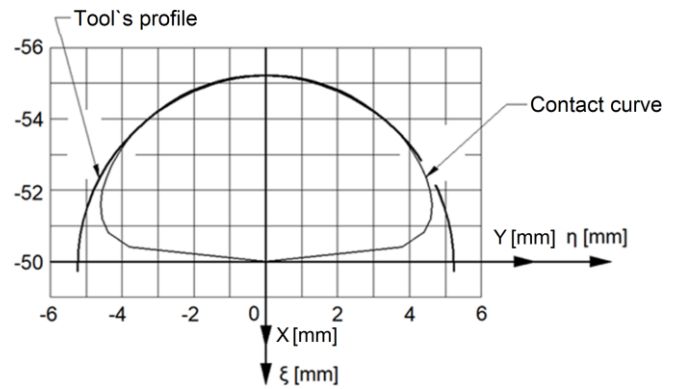
Fig. 3.11. Generator tool profile and contact curve [49]

3.4. Conclusions regarding the development of a tool profiling algorithm that generates by enwrapping - „virtual pole" method

In this chapter, a new complementary method for profiling rack-type tools, gear shaped cutter tool and rotary cutter tool was presented, called the "virtual pole"" method. For these types of tools, the algorithm for applying the method was imagined and dedicated calculation programs were developed to allow the numerical determination of the profile sought.

The "virtual pole" method can be used to profile the tools that generate by enwrapping, by the rolling method and is based on a reinterpretation of the Willis theorem (normals theorem). This starts from the premise that, in order to respect the Willis theorem, when a normal to the profile to be generated passes through the gearing pole, that normal is common for both the profile to be generated and the generating profile. This variant of determining the enveloping condition has the advantage that it avoids the need to write explicitly the equations of the relative movement of the piece with respect to the tool, while remaining scientifically rigorous.

Using the "virtual pole" method greatly simplifies the calculations required for profiling the types of tools mentioned, as determining the relative tool-piece movements is complicated and can be a source of major errors. It should be noted that in the profiling process, the new algorithm does not eliminate the influence of relative movements, but only the need to write these movements explicitly and, therefore, the need to work with relatively complicated equations.

CHAPTER 4. PROFILING OF WORM TOOLS FOR GENERATING SURFACES KNOWN IN ANALYTICAL OR DISCRETE FORM, BY THE „VIRTUAL POLE" METHOD

The numerical representation of a surface can be done in the form of a point cloud.

A first solution for determining the surface is that in which a generator is obtained, a curve known in discrete form and, for a sufficiently large number of points, it can be accepted that it (the generator), together with the guiding curve, accurately models the measured physical surface [50,51].

Another solution is the one in which the surface is modeled with the help of polyhedra whose vertices are represented by the points belonging to the ordered clouds of points.

The proposed profiling algorithm is based on the possibility of analytically expressing surfaces or measuring surfaces and representing them by an ordered point cloud. The algorithm starts from the complementary theorem of the "virtual pole", for profiling rack tool generating a piece that has an ordered curl of profiles.

The methodology is extended from the profiling of rack tool, to the problem of profiling the primary peripheral surface of some worm-type tools, generating the ordered curl of surfaces. This eliminates an important source of errors. The "virtual pole" method has been described in detail in Chapter 3 of this doctoral thesis, respectively in the papers [45] and [46].

4.1. Profiling algorithm of worm tools, by the „virtual pole" method

Figure 4.1 shows the generating with rack tool process, the reference systems, as well as the conjugated axodes.
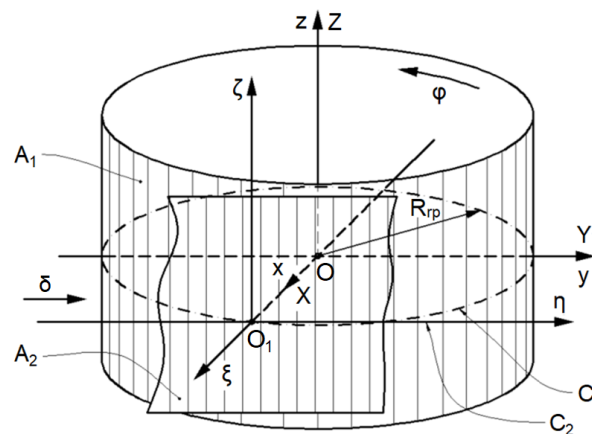
Fig. 4.1. Generating with rack tool. Reference systems and conjugated axodes

It is defined: A_1 - axode of the piece; A_2 - axode of the rack tool; xyz - fixed reference system, having the z axis superimposed on the axode axis A_1; XYZ - mobile reference system, joined with the piece, the Z axis being superimposed on the z axis of the fixed system; $\xi\eta\zeta$ - mobile reference system, joined with the tool. Axoid A_2 belongs to the plane determined by the η and ζ axes. The kinematics of the rolling process of the two axodes respect the rolling condition:

$$\delta = R_{rp} \cdot \varphi, \tag{4.1}$$

where R_{rp} is the rolling radius of the blank and φ is the rotation angle of the reference system associated with the profile to be generated.

Profiling of worm tools for generating surfaces known in analytical or discrete form, by the „virtual pole" method

4.2. Worm tool for processing the disk of a cycloidal reducer

This subchapter presents a new worm tool profiling algorithm for generating the cam of a cycloidal reducer. The algorithm involves determining the active surface of the generating rack, which is reciprocally enwrapping to the active surface of the cycloidal disk [52-55]. The novelty of the algorithm, based on the determination of the intermediate surface, consists in the fact that, for the determination of this surface, the "virtual pole" method is used [45,46]..

Figure 4.2 shows the reference systems used: *xy* represents the fixed reference system, with the origin in point *O*; *XY* - mobile reference system, joined with the piece; *ξη* - the mobile reference system, joined with the tool, with the origin point O_1, as well as the C_1 centrode, associated with the piece and C_2, associated with the tool.

The initial positions of the mobile systems associated with the piece and the tool were denoted by *XY* and *ξη*, and by *X'Y'* and *ξ'η'*, the positions of the same systems, after they were moved, so that the virtual pole, P_v occupies the position of the gearing pole, *P*.

The position represented by a continuous line for *Σ* profile corresponds to the initial moment, while the position represented by a dashed line corresponds to the moment when the virtual pole overlaps the gearing pole. The absolute movements by which the mobile reference systems move are: *I* represents the rotational movement of the *XY* system around point *O* and *II* - the translational movement of the *ξη* system along the *η* axis.
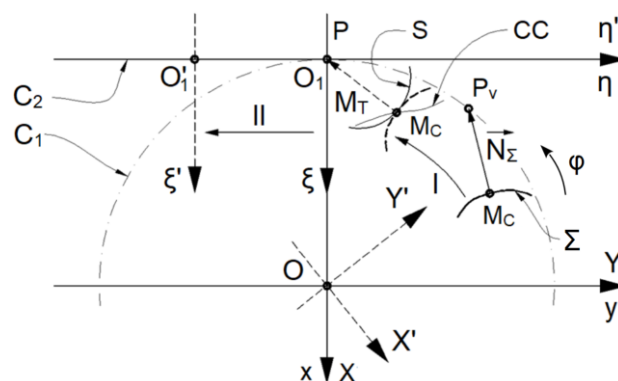
Fig. 4.2. The principle of the virtual pole method

The intersection point between $\vec{N}_\Sigma$ normal taken to the profile to be generated *Σ* and the centrode associated with the piece is the virtual pole P_v. Subsequently, applying to the piece the absolute movement it performs during machining, the virtual pole is brought to the gearing pole, *P*.

In this position, the current point M_C, through which the normal was brought to the profile, is in contact with a point on the tool profile, the M_T point. In addition, the tangency point between the tool profile *S* and the piece profile *Σ*, the point $M_C \equiv M_T$, is currently on the contact curve, *CC*.

Once the intermediate surface of the generating rack is known, its envelope is determined with a cylindrical and constant pitch helical surface, representing the primary peripheral surface of the worm tool.

4.2.1. The equations of the theoretic cycloidal profile

The cycloidal profile is described by a point M, solid with a circle of radius r (radius of the roulette), which rolls outside the base, with a circle of radius R (radius of the base), Figure 4.3 [56]. Four reference systems will be used to identify the cycloidal profile: $X_0Y_0Z_0$ is the reference system in which the coordinates of the *M* point are defined; roulette is defined in this reference system; $X_1Y_1Z_1$ - the reference system with the same origin as the $X_0Y_0Z_0$ system, which rotates

around the Z_0 axis with the angular parameter u (variable parameter describing the piece`s profile); $X_2Y_2Z_2$ - mobile reference system with axles $X_2 \parallel X1$; $Y2 \parallel Y1$; $Z2 \parallel Z1$; XYZ - the mobile reference system, joined with the profile to be generated Σ.

In Figure 4.3, the position indicated by the solid line for roulette corresponds to the initial moment, while the position indicated by dotted line corresponds to a rotation with angle of $v{\neq}0$.
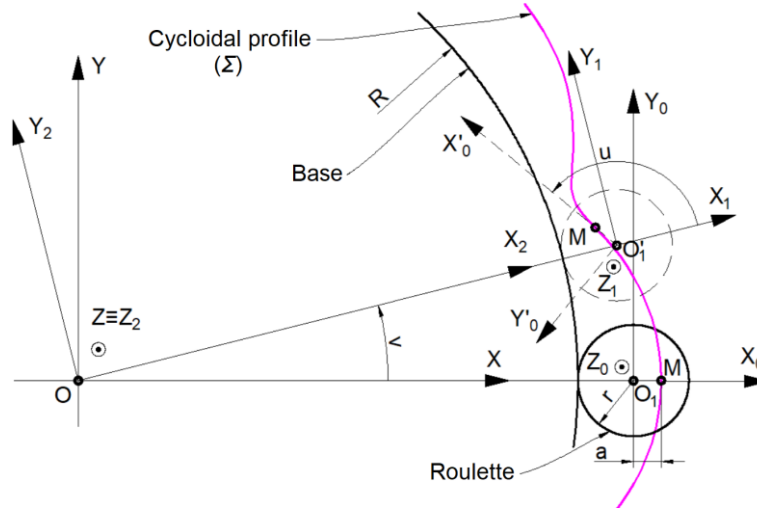
Fig. 4.3. Cycloidal profile generation

The cycloidal profile is a plane curve, therefore, generating this profile and determining the profile of the rack tool, which generates the profile Σ_T, can be treated as a problem of plane enwrapping and can be studied in the XY plan.

Point M has the following coordinates:

$$M: \begin{vmatrix} X_0 = a; \\ Y_0 = 0. \end{vmatrix} \tag{4.2}$$

In the relative movement of system X_0Y_0 to system X_1Y_1, point M describes the circle of equations:

$$M_{X_1Y_1}: \begin{vmatrix} X_1(u) = a \cdot \cos u; \\ Y_1(u) = a \cdot \sin u. \end{vmatrix} \tag{4.3}$$

Therefore, in the X_2Y_2 system, the trajectory of the M point will be a plane curve:

$$M_{X_2Y_2}: \begin{vmatrix} X_2(u) = R + r + a \cdot \cos u; \\ Y_2(u) = a \cdot \sin u. \end{vmatrix} \tag{4.4}$$

The movement of X_2Y_2 system towards to the XY system is given by the relationship developed by the form:

$$\begin{pmatrix} X \\ Y \end{pmatrix} = \begin{pmatrix} \cos v & -\sin v \\ \sin v & \cos v \end{pmatrix} \cdot \begin{pmatrix} R + r + a \cdot \cos u \\ a \cdot \sin u \end{pmatrix} = \begin{pmatrix} (R+r) \cdot \cos v + a \cdot \cos(u+v) \\ (R+r) \cdot \sin v + a \cdot \sin(u+v) \end{pmatrix}. \tag{4.5}$$

Taking into account the rolling condition of the roulette towards to the base, from (4.5) the equations of the cycloidal profile are obtained:

$$\Sigma_T: \begin{vmatrix} X(u) = a \cdot \cos(1+i)u + (R+r) \cdot \cos(i \cdot u); \\ Y(u) = a \cdot \sin(1+i)u + (R+r) \cdot \sin(i \cdot u). \end{vmatrix} \tag{4.6}$$

Profiling of worm tools for generating surfaces known in analytical or discrete form, by the „virtual pole" method

4.2.2. Determining the position of the virtual pole

The normal at the Σ_T profile intersects the circle C_1 of radius R_{rp}, at the distance λ from the current point M of coordinates $X(u), Y(u)$, Figure 4.4 [46].
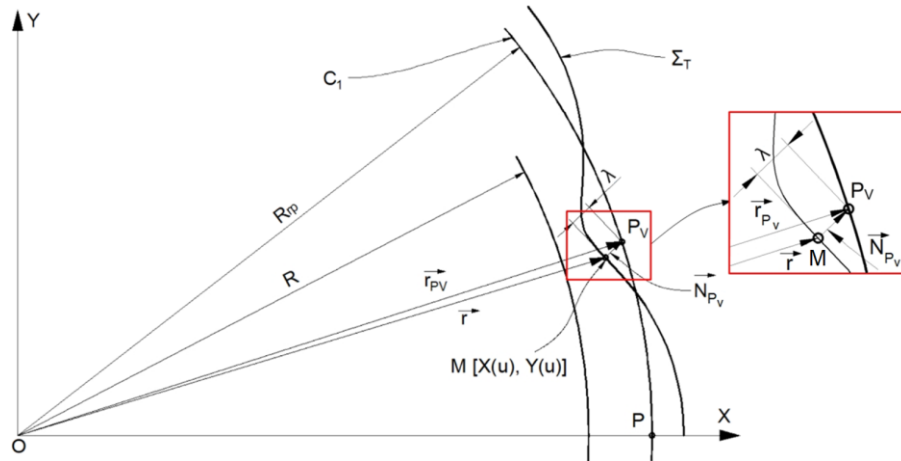
Fig. 4.4. Determining the position of the virtual pole

Therefore, the vector $\vec{N}_{P_v}$ has the equation:

$$\vec{N}_{P_v} = \left[a\cdot(1+i)\cdot cos(1+i)\cdot u + (R+r)\cdot i\cdot cos(i\cdot u)\right]\cdot\lambda\cdot\vec{i} +$$
$$+\left[a\cdot(1+i)\cdot sin(1+i)\cdot u + (R+r)\cdot i\cdot sin(i\cdot u)\right]\cdot\lambda\cdot\vec{j}. \tag{4.7}$$

At the same time, the position vector of the current point M is:

$$\vec{r} = X(u)\cdot\vec{i} + Y(u)\cdot\vec{j} = \left[a\cdot cos(1+i)u + (R+r)\cdot cos(i\cdot u)\right]\cdot\vec{i} +$$
$$+\left[a\cdot sin(1+i)u + (R+r)\cdot sin(i\cdot u)\right]\cdot\vec{j}. \tag{4.8}$$

Thus, the position vector of the P_v point is obtained by summing the vectors $\vec{N}_{P_v}$ and $\vec{r}$:

$$\vec{r}_{P_v} = \vec{N}_{P_v} + \vec{r} = \left\{\left[a\cdot(1+i)\cdot cos(1+i)\cdot u + (R+r)\cdot i\cdot cos(i\cdot u)\right]\cdot\lambda + \right.$$
$$+\left.\left[a\cdot cos(1+i)\cdot u + (R+r)\cdot cos(i\cdot u)\right]\right\}\cdot\vec{i} +$$
$$+\left\{\left[a\cdot(1+i)\cdot sin(1+i)\cdot u + (R+r)\cdot i\cdot sin(i\cdot u)\right]\cdot\lambda + \right.$$
$$+\left.\left[a\cdot sin(1+i)\cdot u + (R+r)\cdot sin(i\cdot u)\right]\right\}\cdot\vec{j}. \tag{4.9}$$

The coordinates of the virtual pole point can be obtained by the form:

$$\left|\begin{array}{l}\left[a\cdot(1+i)\cdot cos(1+i)\cdot u + (R+r)\cdot i\cdot cos(i\cdot u)\right]\cdot\lambda + \\ +\left[a\cdot cos(1+i)\cdot u + (R+r)\cdot cos(i\cdot u)\right] = R_{rp}\cdot cos\varphi; \\ \left[a\cdot(1+i)\cdot sin(1+i)\cdot u + (R+r)\cdot i\cdot sin(i\cdot u)\right]\cdot\lambda + \\ +\left[a\cdot sin(1+i)\cdot u + (R+r)\cdot sin(i\cdot u)\right] = R_{rp}\cdot sin\varphi.\end{array}\right. \tag{4.10}$$

If the parameter λ is removed from the system of equations (4.10), the specific shape of the enwrapping condition is obtained:

$$R_{rp}\cdot a\cdot(1+i)\cdot sin\left[(1+i)\cdot u - \varphi\right] + R_{rp}\cdot(R+r)\cdot i\cdot$$
$$\cdot sin(i\cdot u - \varphi) - (R+r)\cdot a\cdot sin\,u = 0. \tag{4.11}$$

4.2.3. Determining the intermediate surface

The active profile of the cycloidal reducer disk is an equidistant curve to the theoretical cycloid [57,58]. Figure 4.5 shows the theoretical cycloidal profile and the real profile.
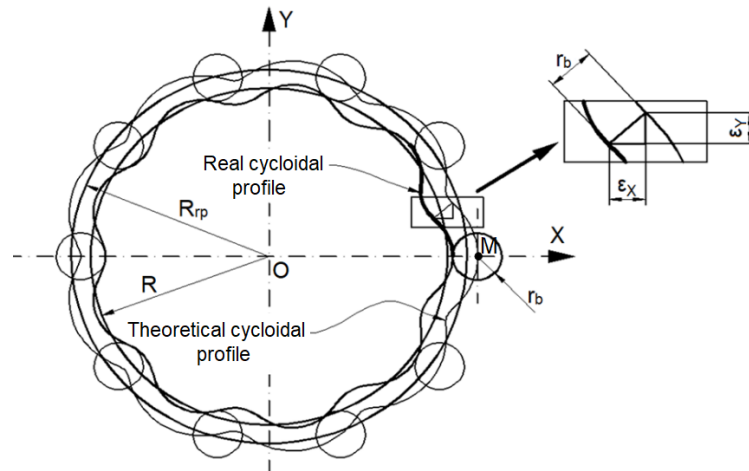
Fig. 4.5. The theoretical cycloidal profile and the real profile

The real profile equations are:

$$\Sigma: \begin{vmatrix} X = X(u) - \varepsilon_X \cdot r_b; \\ Y = Y(u) - \varepsilon_Y \cdot r_b, \end{vmatrix} \tag{4.12}$$

where r_b is the radius of the bolt and ε_X and ε_Y represent the distances between the real and the theoretical profiles.

The coordinates of the current point M are:

$$M: \begin{vmatrix} X_P = X(u) - \varepsilon_X \cdot r_b; \\ Y_P = Y(u) - \varepsilon_Y \cdot r_b. \end{vmatrix} \tag{4.13}$$

If the enwrapping condition is taken into account (4.11), the coordinates of the same point M can be determined when the virtual pole coincides with the gearing pole, therefore, when P belongs simultaneously to the three curves: the profile to be generated, the contact curve (CC) and the generator tool profile (S). The coordinates of the M point on the contact curve, in the fixed reference system, are obtained from the absolute movement of the piece:

$$M_{CC}: \begin{vmatrix} x_P = X_P \cdot \cos\varphi - Y_P \cdot \sin\varphi; \\ y_P = X_P \cdot \sin\varphi + Y_P \cdot \cos\varphi. \end{vmatrix} \tag{4.14}$$

When the parameter u takes values between the limits u_{min} and u_{max}, so that the current point M describes the whole profile Σ, the contact curve, CC, is obtained as:

$$CC: \begin{vmatrix} x(u) = X(u) \cdot \cos\varphi - Y(u) \cdot \sin\varphi; \\ y(u) = X(u) \cdot \sin\varphi + Y(u) \cdot \cos\varphi; \\ \varphi = \varphi(u). \end{vmatrix} \tag{4.15}$$

As in the case of determining the contact curve, the parameter u is assigned a variation between the limits u_{min} and u_{max}, obtaining the equations of the profile of the generating tool:

$$S: \begin{vmatrix} \xi(u) = x(u) + R_{rp}; \\ \eta(u) = y(u) + R_{rp} \cdot \varphi; \\ \varphi = \varphi(u). \end{vmatrix} \tag{4.16}$$

Profiling of worm tools for generating surfaces known in analytical or discrete form, by the „virtual pole" method

The profile was determined using the „virtual pole" method without the need to write the relative movements between the tool and the blank. Of course, the influence of these movements is not undone, but the „virtual pole" method avoids the need to write those movements.

The equations of the intermediate surface are:

$$SI: \begin{vmatrix} \xi(u,t) = x(u) + R_{rp}; \\ \eta(u,t) = y(u) + R_{rp} \cdot \varphi; \\ \zeta(u,t) = t; \\ \varphi = \varphi(u), \end{vmatrix}$$

(4.17)

where t represents an independent variable parameter.

4.2.4. Determining the primary peripheral surface of the generating worm

For determining the primary peripheral surface of the generating worm, it is necessary to determine the characteristic contact curve; meaning the contact curve between the intermediate surface and the helical surface of the worm.

For this purpose, four reference systems will be used, Figure 4.6: $\xi\eta\zeta$ is the reference system joined with the rack, a system in which the intermediate surface is defined; $x_0 y_0 z_0$ - is the reference system joined with the rack, a system in which the intermediate surface is defined; $x_0 y_0 z_0$ - the mobile reference system, having the O_2 origin displaced towards it with the R_{rh} (rolling radius of the worm tool) value; $x_1 y_1 z_1$ - mobile reference system, having the y_1 axis parallel to the $\vec{V}$ axis of the helical surface of the worm; $\xi_1 \eta_1 \zeta_1$ - the reference system joined with the screw tool, having the axis η_1 superimposed on the axis of the screw, $\vec{V}$. In Figure 4.6, the angle θ represents the angle at which the axis of the worm is rotated towards to the η_1 axis, the η_1 axis being parallel to the η axis. This angle represents the rotation angle around the axis x_1.
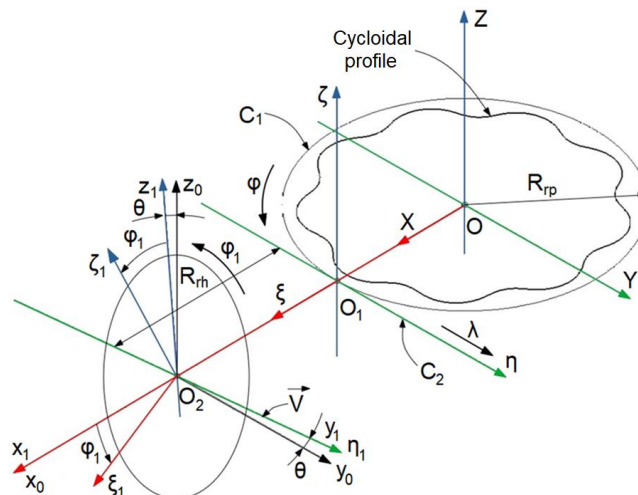
Fig. 4.6. Reference systems used to determine the primary peripheral surface of the generating worm

The coordinate transformation is defined between the coordinate systems $\xi\eta\zeta$ and $x_0 y_0 z_0$:

$$\begin{pmatrix} x_0 \\ y_0 \\ z_0 \end{pmatrix} = \begin{pmatrix} \xi \\ \eta \\ \zeta \end{pmatrix} - \begin{pmatrix} -R_{rh} \\ 0 \\ 0 \end{pmatrix}.$$

(4.18)

in which R_{rh} represents the rolling radius of the worm, being a constructive size.

The generator S of the intermediate surface SI is discreetly known as:

$$S = \begin{pmatrix} \xi_1 & \eta_1 \\ \vdots & \vdots \\ \xi_i & \eta_i \\ \vdots & \vdots \\ \xi_n & \eta_n \end{pmatrix}.$$

(4.19)

The intermediate surface SI will be approximated with a surface family of the plane stripe type, determined by displacing the segments $\xi_i \eta_i$ along a direction parallel with the ζ axis, Figure 4.7.
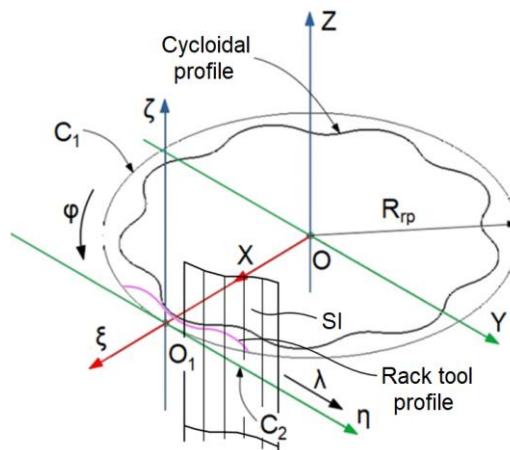
Fig. 4.7. Aproximarea suprafeței intermediare

In this way, the intermediate surface can be approximated by a point cloud known in discrete form:

$$SI_a : \begin{vmatrix} \xi = \xi_i + u_1 \cdot \cos \alpha_i; \\ \eta = \eta_i + u_1 \cdot \sin \alpha_i; \\ \zeta = h_i, \end{vmatrix}$$

(4.20)

where SI_a represents the approximate intermediate surface of the point cloud known in discrete form, u_1 and h_i are independent variable parameters, and αi represents the inclination angle of the segment approximating the profile of the rack tool.

The normal to the approximated surface, taken in any of its known points, will have the form:

$$\vec{N} : \begin{vmatrix} \xi = \xi_i + u_1 \cdot \sin \alpha_i; \\ \eta = \eta_i - u_1 \cdot \cos \alpha_i; \\ \zeta = h_i. \end{vmatrix}$$

(4.21)

At the same time, the $\vec{V}$ axis of the helical surface in the $\xi \eta \zeta$ system has the form:

$$\vec{V} : \begin{vmatrix} \xi = -R_{rh}; \\ \eta = t \cdot \cos \theta; \\ \zeta = -t \cdot \sin \theta, \end{vmatrix}$$

(4.22)

with t independent parameter and θ the inclination angle of the worm curl.

Profiling of worm tools for generating surfaces known in analytical or discrete form, by the „virtual pole" method

From the equations (4.21) and (4.22) the coordinates of the intersection point between the normal to the approximate intermediate surface, $\vec{N}$ and the axis of the helical surface $\vec{V}$, can be determined:

$$\vec{N} \cap \vec{V} : \begin{vmatrix} \xi = \xi_i + u_1 \cdot \sin\alpha_i = -R_{rh}; \\ \eta = \eta_i - u_1 \cdot \cos\alpha_i = t \cdot \cos\theta; \\ \zeta = h = -t \cdot \sin\theta. \end{vmatrix} \qquad (4.23)$$

When $i = 1 \div n$, the characteristic curve in discrete form, CC_m, can be determined:

$$CC_m = \begin{pmatrix} \xi_1 & \eta_1 & \zeta_1 \\ \vdots & \vdots & \vdots \\ \xi_i & \eta_i & \zeta_i \\ \vdots & \vdots & \vdots \\ \xi_n & \eta_n & \zeta_n \end{pmatrix}. \qquad (4.24)$$

The equation of the primary peripheral surface of the worm tool can be written in developed form:

$$S_M: \begin{vmatrix} \xi_1 = (\xi - R_{rh}) \cdot \cos\varphi_1 - (\eta \cdot \sin\theta - \zeta \cdot \cos\theta) \cdot \sin\varphi_1; \\ \eta_1 = \eta \cdot \cos\theta + \zeta \cdot \sin\theta + p_e \cdot \varphi_1; \\ \zeta_1 = -(\xi - R_{rh}) \cdot \sin\varphi_1 - (\eta \cdot \sin\theta - \zeta \cdot \cos\theta) \cdot \cos\varphi_1. \end{vmatrix} \qquad (4.25)$$

Therefore, the axial section of the primary peripheral surface of the worm tool is obtained:

$$SA: \begin{vmatrix} \xi_1 = (\xi - R_{rh}) \cdot \cos\varphi_1 - (\eta \cdot \sin\theta - \zeta \cdot \cos\theta) \cdot \sin\varphi_1; \\ \eta_1 = \eta \cdot \cos\theta + \zeta \cdot \sin\theta + p \cdot \varphi_1; \\ \zeta_1 = -(\xi - R_{rh}) \cdot \sin\varphi_1 - (\eta \cdot \sin\theta - \zeta \cdot \cos\theta) \cdot \cos\varphi_1; \\ \varphi_1 = \arctan\left(\dfrac{\eta \cdot \sin\theta - \zeta \cdot \cos\theta}{R_{rh} - \xi} \right). \end{vmatrix} \qquad (4.26)$$

4.2.5. Numerical application - Worm tool for generating the disk of a cycloidal reducer

A numerical application was made for the profiled disk of a cycloidal reducer. The disk has the dimensions presented in table 4.1, with the following notations: R - radius of the base; r - radius of the roulette; a - the distance between the generating point of the cycloid and the center of the roulette; r_b - radius of the bolts; R_{rp} - rolling radius of the blank; R_{rh} - rolling radius of the worm (value chosen constructively).

Table 4.1. The dimensions of the profiled disk in the composition of a cycloidal reducer

R [mm]	r [mm]	a [mm]	r_b [mm]	R_{rp} [mm]	R_{rh} [mm]
36	4	2	5	40	60

The calculation application was developed in the Octave program, a software product designed for performing numerical calculations. By running the calculation program was obtained the theoretical profile of the cycloid, the equidistant curve to this profile and the profile of the generating rack tool, Figure 4.8.

Table 4.2 shows the coordinates of the points belonging to the profile to be generated and of the points belonging to the profile of the generating rack tool. In order to demonstrate the accuracy of identifying the solution for the enwrapping condition, in the same table, for each value of the variable u, the value of this condition is given, found using the "*fzero*" function.
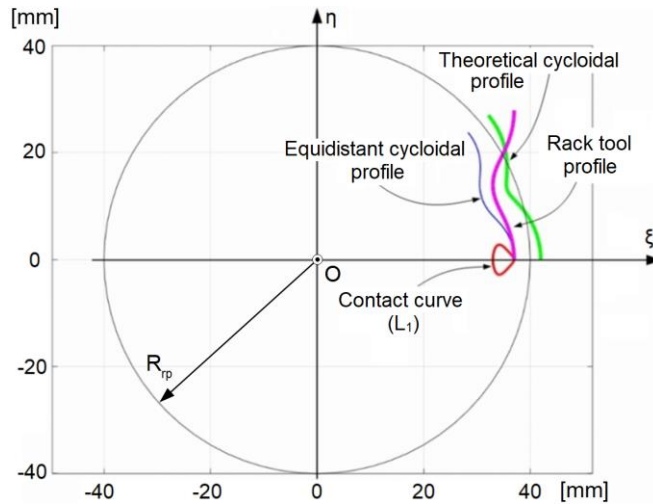
Fig. 4.8. Theoretical cycloid, equidistance at it, contact curve and the profile of the rack tool

Table 4.2. The coordinates of the points belonging to the profile to be generated and the rack tool profile

Crt. no.	u [rad]	X [mm]	Y [mm]	ξ [mm]	η [mm]	Enwrapping condition
1	0	37	0	-3	0	0
2	0,873	36,298	3,671	-3,528	4,120	0
3	1,745	34,669	6,397	-4,819	7,607	0
4	2,618	32,569	8,689	-6,384	10,895	$4{,}97 \cdot 10^{-14}$
5	3,141	31,010	11,287	-7	13,963	$-2{,}85 \cdot 10^{-14}$
6	3,665	30,534	14,279	-6,384	17,030	$6{,}39 \cdot 10^{-14}$
7	4,538	30,670	17,384	-4,819	20,318	$8{,}53 \cdot 10^{-14}$
8	5,410	30,166	20,520	-3,528	23,805	$-1{,}71 \cdot 10^{-13}$
9	6,283	28,343	23,783	-3	27,925	$1{,}95 \cdot 10^{-13}$

Figure 4.9 shows the intermediate surface of the generating rack, the primary peripheral surface of the worm and the characteristic curve, and table 4.3 shows the coordinates of some of the points belonging to the characteristic curve and the axial section of the worm. If the contact curve between the active surface of the cycloidal disk and the intermediate surface is denoted by L_1 (Figure 4.8) and the contact curve between the intermediate surface and the primary peripheral surface of the worm tool is denoted by L_2 (Figure 4.9), the intersection point of the two curves represents the characteristic point, meaning the contact point between the cylindrical surface of the cycloidal disk and the primary peripheral surface of the worm tool.
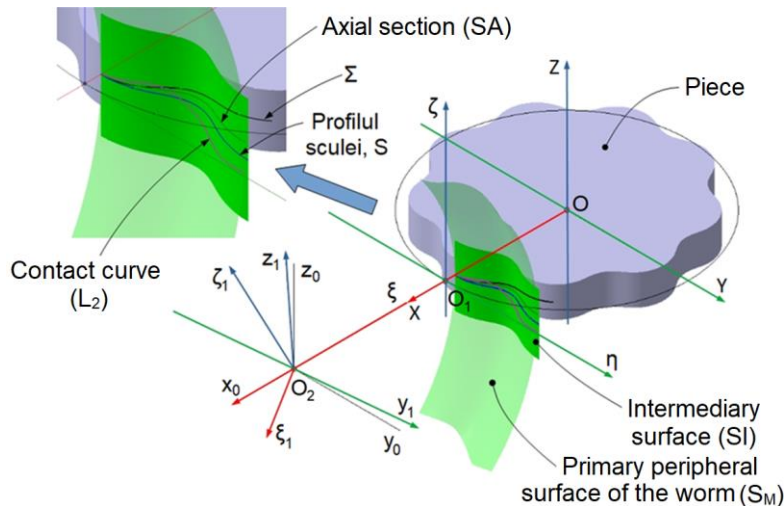
Fig. 4.9. Intermediate surface, primary peripheral surface and characteristic curve

Profiling of worm tools for generating surfaces known in analytical or discrete form, by the „virtual pole" method

Table 4.3. The coordinates of the points on the characteristic curve and the axial section

Crt. no.	Characteristic curve			Axial section		
	ξ_1 [mm]	η_1 [mm]	ζ_1 [mm]	ξ_1 [mm]	η_1 [mm]	ζ_1 [mm]
1.	-53,000	0,010	0,109	-53,000	0,001	0,000
2.	-53,528	4,175	0,437	-53,530	4,139	0,000
3.	-54,820	7,690	0,592	-54,823	7,642	0,000
4.	-56,384	10,883	-0,616	-56,387	10,932	0,000
5.	-57,000	13,772	-2,765	-57,067	13,987	0,000
6.	-56,384	16,683	-4,659	-56,576	17,049	0,000
7.	-54,820	19,916	-5,425	-55,087	20,354	0,000
8.	-53,528	23,439	-5,176	-53,778	23,867	0,000
9.	-53,022	26,746	-4,903	-53,248	27,156	0,000

The axial section of the generating worm, obtained by applying the equations (4.26), is shown in Figure 4.10.
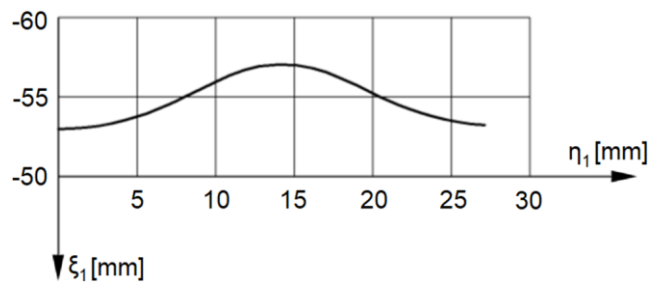
Fig. 4.10. The axial section of the generating worm

4.3. Profiling of the worm tool generating an orderly curl, known in discrete form
4.3.1. The substitutive point cloud of generating surface

Figure 4.11 shows the reference systems: *XOY* represents the mobile reference system, joined with the piece profile; *xOy* - fixed reference system; *ξO₁η* - mobile reference system, joined with the tool profile. The *S* surface is the primary peripheral surface of the generating tool and is unknown at the initial moment. The *Σ* surface is the surface to be generated and is modeled (substituted) by a cloud of points whose coordinates were determined by scanning [50].
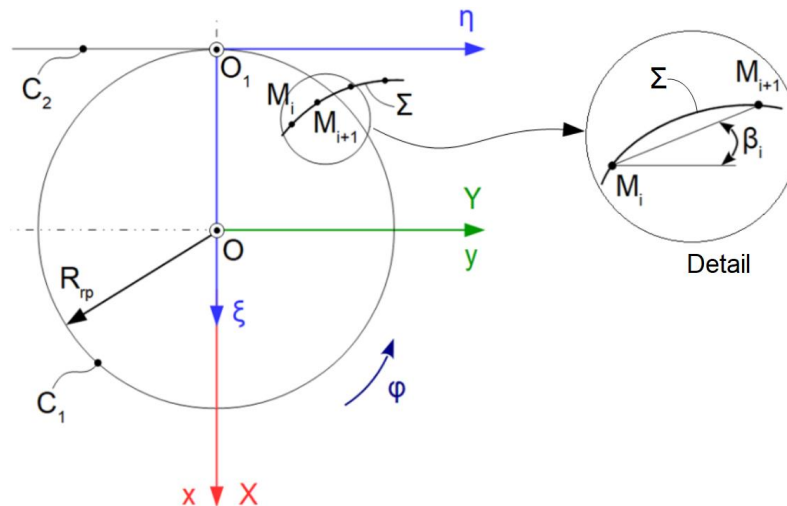
Fig. 4.11. *C₁* and *C₂* centrodes and the approximation of the *Σ* curve [50]

The *Σ* curve can be discreetly modeled by the point cloud [50]:

$$\Sigma : \begin{pmatrix} X_1 & Y_1 \\ X_2 & Y_2 \\ \vdots & \vdots \\ X_n & Y_n \end{pmatrix}. \tag{4.27}$$

The $M_i M_{i+1}$ segment can be expressed in parametric form by [50]:

$$\Sigma_{i,i+1} : \begin{vmatrix} X(u) = X_i + u \cdot \sin\beta_i; \\ Y(u) = Y_i + u \cdot \cos\beta_i, \end{vmatrix} \qquad i = 1, ..., n, \tag{4.28}$$

with u scalar parameter variable between limits $u_{min} = 0$, $u_{max} = \beta_i$ and $tg\beta_i = \dfrac{Y_i - Y_{i+1}}{X_i - X_{i+1}}$.

The equations (4.28) determines the elementary profile $\Sigma_{i,\,i+1}$ substitutive of the generating curve [50].

4.3.2. Discretization of the profile to be generated

For a discrete known profile, Figure 4.12 shows the cycloidal disk as part of a cycloidal reducer whose coordinates were determined by scanning using *Atos Core* equipment. In order to determine the profile to be generated, in the *GOM Inspect* program, equidistant points were considered on one of the lobes of the disk of the cycloidal profile, located at a distance of 2 mm between them, using the command *Equidistant Points* ⸬.
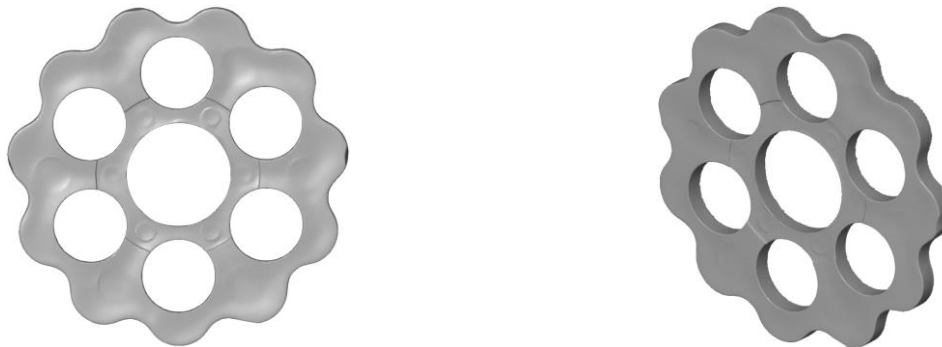
Fig. 4.12. Disk from a cycloidal reducer

The coordinates of these points were exported to a **.csv* file, so that they could be used later in the *Octave* program to determine the profile of the generating tool and the contact curve.

The parametric equations of the C_1 centrode, Figure 4.11, are [50]:

$$C_1 : \begin{vmatrix} X = -R_{rp} \cdot \cos\varphi; \\ Y = R_{rp} \cdot \sin\varphi, \end{vmatrix} \tag{4.29}$$

R_{rp} being the rolling radius of the piece (the radius of the outer circle of the curls ordered by the *Σ* profiles can be accepted as the size of the R_{rp} radius) and φ is the angular parameter that defines the rotation of the reference system joined with the piece around the *Z* axis.

The condition for determining the virtual pole is by the form:

$$\begin{vmatrix} -R_{rp} \cdot \cos\varphi = X_i + \lambda \cdot \dot{Y}_u; \\ R_{rp} \cdot \sin\varphi = Y_i - \lambda \cdot \dot{X}_u, \end{vmatrix} \tag{4.30}$$

Profiling of worm tools for generating surfaces known in analytical or discrete form, by the „virtual pole" method

or after successive processing [50]:

$$\lambda = \frac{-R_{rp} \cdot cos\,\varphi - X_i}{\dot{Y}_u} = \frac{-R_{rp} \cdot sin\,\varphi + Y_i}{\dot{X}_u} \Rightarrow \left(-R_{rp} \cdot cos\,\varphi - X_i\right) \cdot \dot{X}_u = \left(-R_{rp} \cdot sin\,\varphi + Y_i\right) \cdot \dot{Y}_u \Rightarrow$$

$$\Rightarrow \left(-R_{rp} \cdot sin\,\varphi + Y_i\right) \cdot \dot{Y}_u + \left(R_{rp} \cdot cos\,\varphi + X_i\right) \cdot \dot{X}_u = 0 \Leftrightarrow \left(R_{rp} \cdot cos\,\varphi + X_i\right) \cdot \dot{X}_u - \hfill (4.31)$$

$$-\left(R_{rp} \cdot sin\,\varphi - Y_i\right) \cdot \dot{Y}_u = 0,$$

for $\left(X_i, Y_i\right)$ $i = 1,...,n.$

Basically, the gearing curve is defined in the fixed reference system, in the form [50]:

$$CA: \begin{vmatrix} x = x(u,\varphi); \\ y = y(u,\varphi); \\ \varphi = \varphi(u). \end{vmatrix} \hfill (4.32)$$

By transferring the points on the gearing curve into the tool-associated system, *ξη*, the side of the generating rack is determined. For this, the absolute movement is imprinted on the points on the gearing curve [50]:

$$\xi = x + A; \quad A = \begin{pmatrix} -R_{rp} \\ -R_{rp} \cdot \varphi \end{pmatrix}. \hfill (4.33)$$

4.3.3. Numerical application - Worm tool for generating a known in discrete form profile

A numerical application for profiling the worm tool has been developed to process a profile known in discrete form. The rolling radius of the piece is the outer diameter of the cycloidal disk, determined by scanning, R_{rp}=33 mm.

Table 4.4 shows the coordinates of the profile of the rack tool and the profile of the piece.

Table 4.4. The coordinates of the profile of the rack tool and the profile of the piece

Crt. no.	Tool profile		Piece profile		Crt. no.	Tool profile		Piece profile	
	ξ [mm]	η [mm]	X [mm]	Y [mm]		ξ [mm]	η [mm]	X [mm]	Y [mm]
1	3,972	-8,785	28,070	-7,500	11	0,162	0,714	32,830	0,710
2	3,664	-7,816	28,640	-6,680	12	0,316	1,718	32,640	1,700
3	3,116	-6,877	29,370	-5,990	13	0,593	2,696	32,300	2,640
4	2,415	-5,976	30,160	-5,390	14	0,982	3,642	31,830	3,510
5	1,725	-5,086	30,930	-4,750	15	1,516	4,573	31,210	4,300
6	1,151	-4,184	31,600	-4,010	16	2,167	5,467	30,480	4,980
7	0,716	-3,240	32,130	-3,160	17	2,842	6,323	29,690	5,600
8	0,393	-2,270	32,530	-2,240	18	3,400	7,206	28,960	6,280
9	0,195	-1,288	32,780	-1,280	19	3,779	8,144	28,360	7,070
10	0,119	-0,281	32,880	-0,280	20	-	-	27,940	7,980

Figure 4.13 shows the profile of the generating tool made in the *Octave* program - the green curve represents the piece profile, the blue one represents the contact curve, and the red one represents the profile of the rack tool [50].

The axial section of the worm tool is obtained from the relation (4.26), Figure 4.14.

The coordinates of the points on the characteristic curve and the axial section are shown in table 4.5.
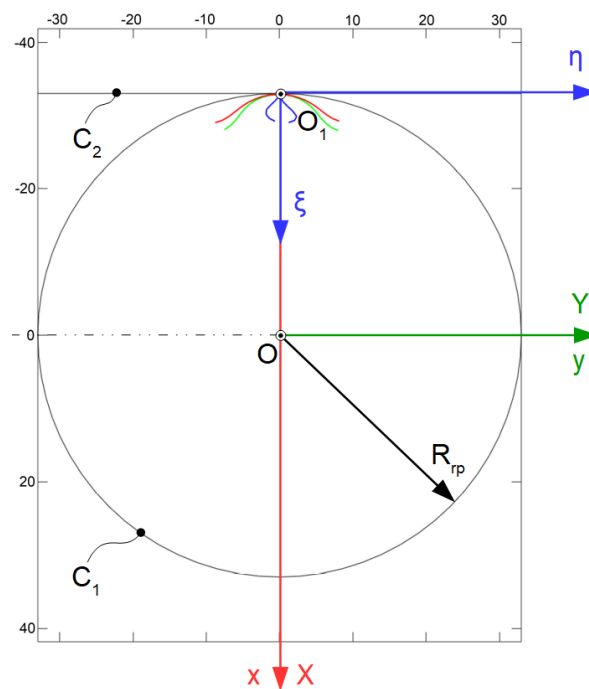
Fig. 4.13. The profile of the generating tool and the contact curve

Table 4.5. The coordinates of the points on the characteristic curve and the axial section

Crt. no.	Characteristic curve			Axial section		
	ξ_1 [mm]	η_1 [mm]	ζ_1 [mm]	ξ_1 [mm]	η_1 [mm]	ζ_1 [mm]
1	-46,870	6,646	-1,779	-46,696	-7,227	0,000
2	-47,914	5,242	-2,220	-47,744	-5,863	0,000
3	-48,892	3,802	-1,549	-48,732	-4,454	0,000
4	-49,549	2,201	-0,855	-49,429	-2,883	0,000
5	-49,857	0,475	-0,217	-49,817	-1,209	0,000
6	-49,803	-1,281	0,414	-49,856	0,509	0,000
7	-49,365	-2,969	1,077	-49,570	2,204	0,000
8	-48,606	-4,498	1,823	-48,960	3,811	0,000
9	-47,523	-5,927	2,289	-48,049	5,269	0,000
10	-46,548	-7,319	1,578	-46,993	6,628	0,000
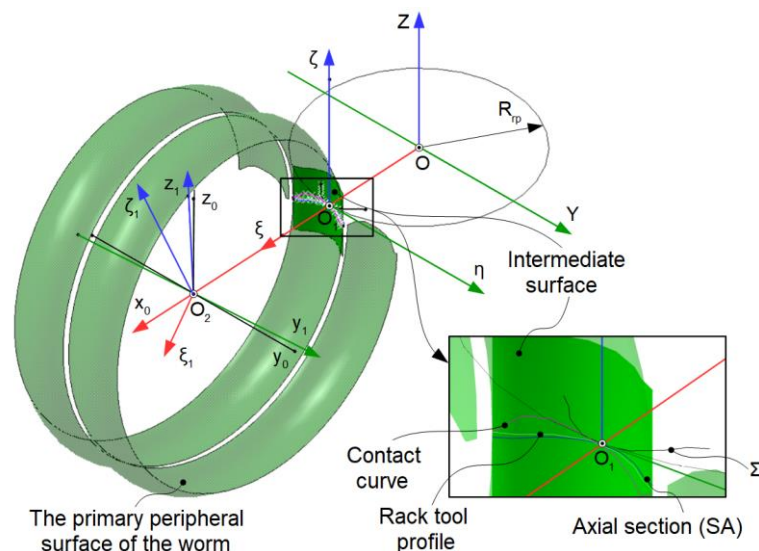
Fig. 4.14. The primary peripheral surface of the worm and the axial section

The axial section of the worm tool is shown in Figure 4.15.
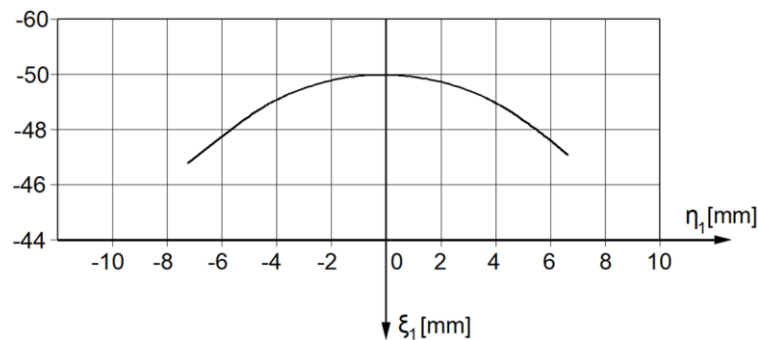
Fig. 4.15. The axial section of the worm tool

4.4. Conclusions regarding the profiling of worm tools for generating surfaces known in analytical or discrete form, by the „virtual pole" method

In this chapter was presented a new worm tool profiling algorithm for generating the active surface of the cam of a cycloidal reducer (algorithm based on determining the intermediate surface of the generating rack, which is reciprocally enveloping to the surface of the cycloidal disk).

The novelty of the algorithm is that it is use an innovative method of determining this surface, a method called the „virtual pole" method.

The „virtual pole" method has been described in detail in Chapter 3 of this doctoral thesis, entitled „Development of a tool profiling method that generates by enwrpping by the rolling method - „virtual pole" method".

This method allows to determine the profile of the generating tool without the need to write the relative movements between the tool and the blank.

Of course, the influence of these movements is not undone, but the „virtual pole" method avoids the need to write those movements, which are described by complicated equations that increase the risk of error.

The intermediate surface will be approximated with a family of plane stripe type surfaces, determined by approximating the generating curve with a point cloud.

At the same time, in the chapter was presented a variant for determining the enwrapping condition in the case of the worm tool intended for processing a profile known in discrete form, namely, the cycloidal disk in the composition of a cycloidal reducer.

The calculation time for tool profiling is thus significantly reduced and the disadvantage of the resulting error, which is small enough to be technically acceptable, is fully compensated by this reduction of calculation time.

CHAPTER 5. IMPLEMENTATION OF THE „VIRTUAL POLE" METHOD FOR THE STUDY OF THE ENWRAPPING SURFACES DETERMINED BY REVERSE ENGINEERING TECHNIQUES

In this chapter, it is proposed to redesign four types of pieces (two parts pieces of a helical pump (driver and driven screws) and two worm shafts in the construction of the seats adjustment mechanism of Audi and Mercedes cars) according to the numerical models obtained by scanning. These models are obtained based on the processing of point clouds resulting from the 3D scanning of the respective pieces.

After completing the actual scanning process, the pieces were measured using a specific software (*GOM Inspect*), in order to establish their dimensional characteristics, and their modeling was done in a computer aided design program (*CATIA V5R21*).

Subsequently, the inspection was performed, by overlapping the scanned model and the CAD model of each piece, in order to compare the analytical models with the real pieces. This comparison allows to appreciate the degree to which the analytical model obtained by redesign corresponds to the real piece.

In this way, the ability of future pieces, obtained on the basis of the analytical model, to be able to fulfill the desired functional role can be appreciated. The inspection can provide information about the deviations of the pieces from the theoretical models. These deviations can be analyzed for the entire piece or for its functional surfaces.

5.1. 3D scanning of helical surfaces

The four pieces with helical surfaces are scanned with the Atos Core device, Figure 5.1, an equipment produced by the GOM company from Germany [59]. The equipment is existing in the Department of Manufacturing Engineering, within the Faculty of Engineering, "Dunărea de Jos" University of Galați.

Fig. 5.1. Atos Core scanner [60,61]

The processing of the images after scanning is done through the *GOM Scan* software. *GOM Scan* is an easy-to-use and intuitive scanning software, a solution dedicated to the fields of reverse engineering and rapid protyping.

Using the *Scan* command in the *Acquisition -> Measurement* module, the actual scanning process is performed. During scanning, the software projects different line patterns onto the object surface. The software immediately displays the surface data captured in the 3D view. The sensor only captures what it can see with both cameras.

Implementation of the „virtual pole" method for the study of the enwrapping surfaces determined by reverse engineering techniques

5.1.1. Scanning of the active components from a helical pump

The driver screw and the driven screw are shown in Figures 5.2 and 5.3.

Fig. 5.2. The driver screw from a helical pump

Fig. 5.3. The driven screw from a helical pump

In order to begin the scanning process, reference markers must be applied to the pieces, Figure 5.4, so that they can be recognized by the scanning equipment and software..
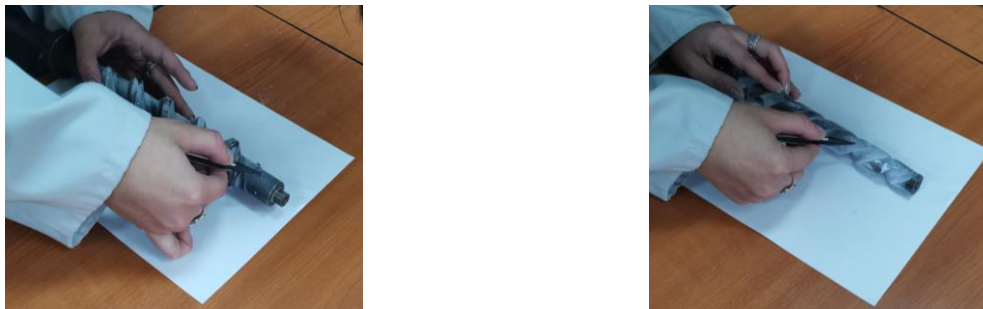
Fig. 5.4. Application of the reference markers on the driver screw and the driven screw

To ensure high scanning accuracy, it is necessary to apply an anti-reflective spray to the pieces so that the glossy surfaces of the pieces to become matte surfaces, because glossy surfaces generally lead to poor scanning quality.

After applying the reference markers and the anti-reflective spray, the actual scanning process of the driver and driven screws begins, Figura 5.5.
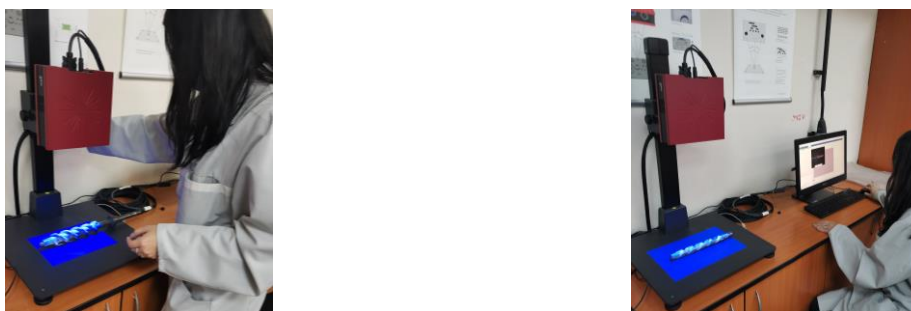
Fig. 5.5. Scanning of the two screw from a helical pump

Multiple scans from different angles are required to fully scan an object. The software lists all scans in a single set of measurements. Finally, 23 scan steps resulted for the driver screw and 16 scan steps for the driven screw. After scanning the pieces, the polygonalization process begins, which consists in correlating all the scans of the elements and obtaining the complete numerical model. Thus, from the GOM Scan menu, it is chosen: *Acquisition -> Measurement series -> Polygonize and Recalculate* and the network of the points provided on the surface of the pieces will be calculated.

The imperfections and the unwanted edges on the scanned pieces will be removed with the *Select/Deselect Through Surface* ⊹ command. Therefore, Figure 5.6 shows the final model of the driver screw, and Figure 5.7 shows the final model of the driven screw, scanned using the Atos Core equipment.
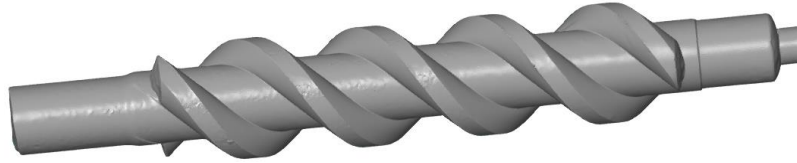
Fig. 5.6. Scanned driver screw model of a helical pump
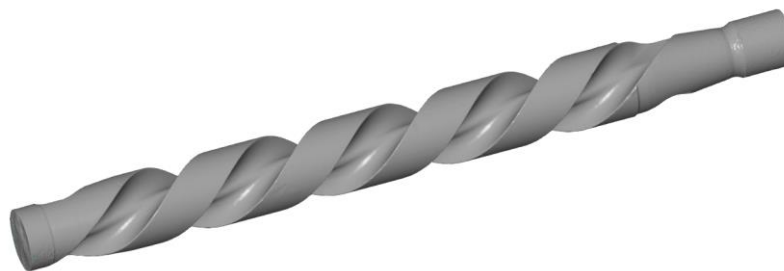
Fig. 5.7. Scanned driven screw model of a helical pump

Scanned pieces will be saved in **.stl* format, allowing them to be opened in various software design programs, such as Autodesk Inventor, CATIA, SolidWorks, AutoCAD, etc.

5.1.2. Scanning of worm shafts from the construction of worm gears-worm wheel

The scanning process of two worm shafts in the construction of the seats adjustment mechanism of of Audi and Mercedes cars is similar to scanning the driver screw and the driven screw of a helical pump.

The two worm shafts are shown in Figures 5.8 and 5.9.

Fig. 5.8. The worm shaft from the construction of the seat adjustment mechanism of an Audi car

Fig. 5.9. The worm shaft from the construction of the seat adjustment mechanism of a Mercedes car

The reference markers, in the case of worm shafts, are applied both to the table of the scanning equipment and to the pieces, so that they can be recognized by the software as reference points. Then, the anti-reflective spray will be applied on both pieces.

Finally, after the scanning process, for the worm shaft from the construction of the seat adjustment mechanism of an Audi car, were resulted 64 scanning steps and for the worm shaft from the construction of the seat adjustment mechanism of a Mercedes car, were resulted 52 scanning steps.

Implementation of the „virtual pole" method for the study of the enwrapping surfaces determined by reverse engineering techniques

Following the polygonalization process, figures 5.10 and 5.11 show the final Following the polygonalization process, figures 5.10 and 5.11 show the final models of the worm shafts in the construction of the seats adjustment mechanism of Audi and Mercedes cars..
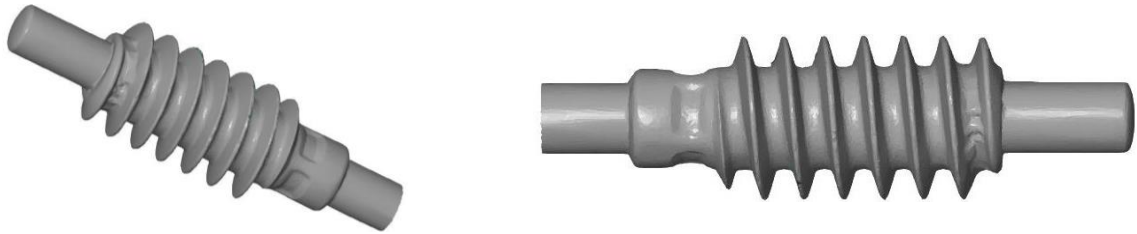
Fig. 5.10. The scanned model of the worm shaft from the construction of the seat adjustment mechanism of an Audi car

Fig. 5.11. The scanned model of the worm shaft from the construction of the seat adjustment mechanism of a Mercedes car

As in the case of driver and driven screws, the two scanned worm shafts will be saved in *.stl* format, allowing them to be opened in various design programs, such as Autodesk Inventor, CATIA, SolidWorks, AutoCAD, etc.

5.2. Inspection of the active components from a helical pump

The inspection of the driver and driven screws is performed through the *GOM Inspect* program, to establish their dimensional characteristics. Thus, the contour of the two pieces from a helical pump was constructed, using the *Single Section* command, having as reference plane a plane parallel to the axis of a cylinder previously built in the inspection program.

By means of the contours, the dimensions of the pieces can be determined. For example:
a. to determine the maximum length, two points positioned at the ends of the driver and driven screws using the Point command are chosen, and by the *2-Point Distance* •–• command, from the *Construct -> Distance* 🔲 module, the maximum length of the pieces can be measured, Figure 5.12;
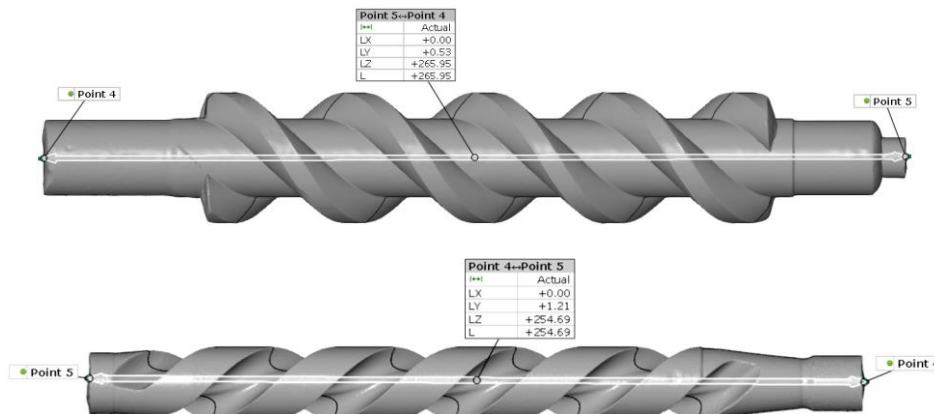
Fig. 5.12. Measuring the maximum length of the driver screw and the driven screw

b. to determine the inner and outer diameter of the driver and driven screws, a circle on the front profile is construct, using the *Fitting Circle* ⊙ command from *Construct -> Circle* ○ module, Figure 5.13;
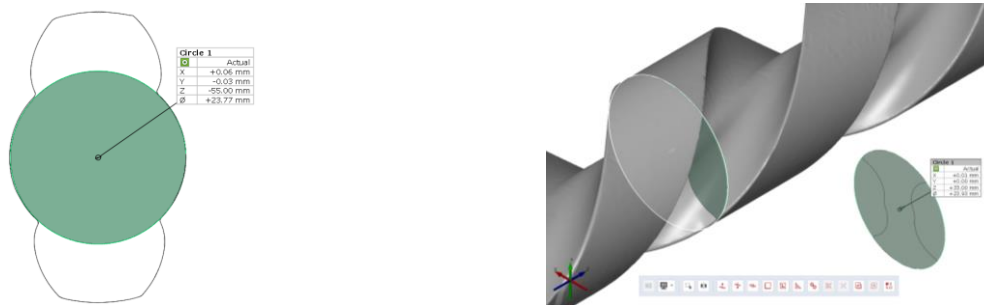
Fig. 5.13. Determining the inner and outer diameter of the driver and driven screws

c. in order to determine the coordinates of points belonging to the front profiles of the pieces, equidistant points are generated on their contour, using the *Point* command, which will be built into the modeling software, Figure 5.14.
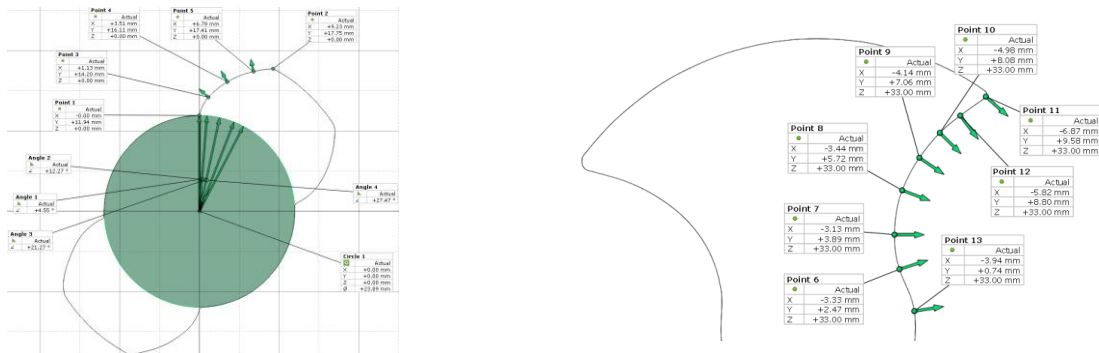
Fig. 5.14. Construction of points in order to determine the form of the front profile of the driver and driven screws

5.3. Study of the enwrapping of the active surfaces of helical pump elements by analyzing the frontal profiles using the „virtual pole" method

After the polygonalization of the point cloud obtained by scanning, the numerical model obtained was aligned, choosing a reference system that would allow the identification of points belonging to the front profile of the screw as easy as possible, Figure 5.15.

a.   b.
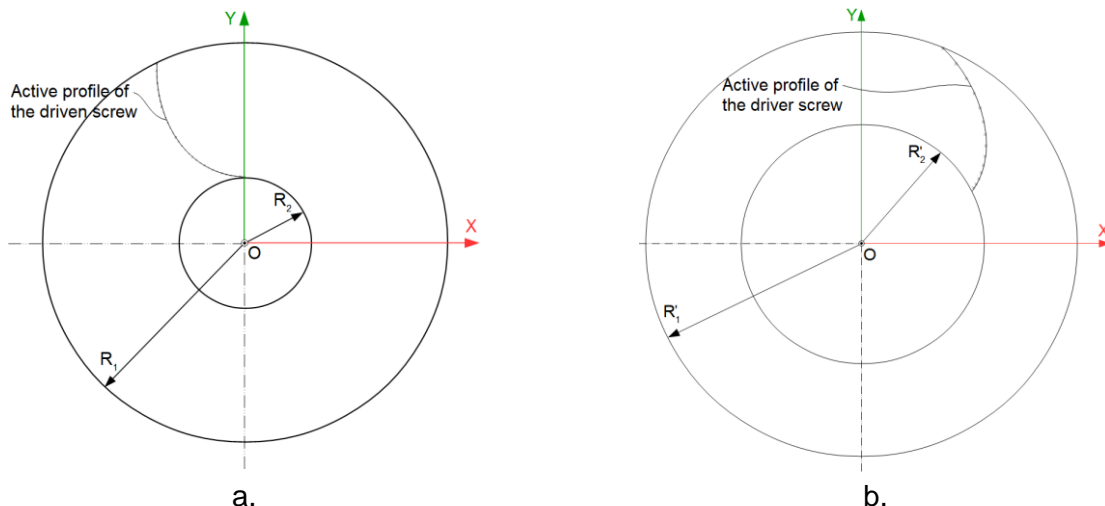
Fig. 5.15. Front active profile of: a. driven screw; b. driver screw.

Implementation of the „virtual pole" method for the study of the enwrapping surfaces determined by reverse engineering techniques

By measuring the scanned surfaces, the values were obtained: $R_1=12$ mm; $R_2=4$ mm. Similar measurements were made for the driver screw, obtaining: $R_1^{'}=20$ mm; $R_2^{'}=12$ mm.

According to the data from literature [62,63], the active flank of the helical surface of the driven screw is an epicycloid obtained by rolling on the base circle of radius $R_1=12$ mm of the circle of roulette radius $R_2^{'}=12$ mm. The point that generates the epicycloid is at a distance $a=\left(R_1+R_2^{'}-R_2\right)$ from the center of the roulette. In this case, $R_1 = R_2^{'} = R$.

According to the presented data, the parametric equations of the front profile of the driven screw are:

$$\Sigma: \begin{vmatrix} X = 2 \cdot R \cdot \sin u - a \cdot \sin(2 \cdot u); \\ Y = 2 \cdot R \cdot \cos u - a \cdot \cos(2 \cdot u), \end{vmatrix} \tag{5.1}$$

where *u* represents a variable parameter that describes the pieces profile.

The active profiles of the two screws are reciprocally enwrapping curves. Therefore, their frontal envelope can be studied by known methods [2,4,51], in particular by the "virtual pole" method. According to the "virtual pole" method, the identification of the profile of the driver rotor, reciprocally enwrapping the profile known by equations (5.1), involves the consideration of four reference systems, Figure 5.16: *xy* - fixed reference system, with the origin in the center of the driven screw rolling circle, C_1 circle; x_0y_0 - fixed reference system, with the origin in the center of the rolling circle of the driver screw, C_2 circle; X_1Y_1 - mobile reference system, joined with the driven screw; X_2Y_2 - mobile reference system, joined with the driver screw.
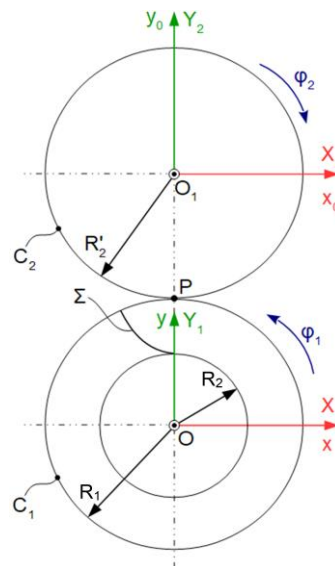
Fig. 5.16. Establishment of the reference systems to identify the profile of the driver screw

Between the reference systems *xy* and x_0y_0, the coordinate transformation relationship can be established:

$$x_0 = x + A; \quad A = \begin{pmatrix} 0 \\ -A_{12} \end{pmatrix}; \quad A_{12} = R_1 + R_2^{'} = 2 \cdot R. \tag{5.2}$$

According to known algorithms for the study of enwrapping curves [2,4,51], the two mobile reference systems have the absolute movements:

$$x = \omega_3^T\left(\varphi_1\right) \cdot X \text{ și } x_0 = \omega_3^T\left(-\varphi_2\right) \cdot X_1. \tag{5.3}$$

The same algorithms [2,4,51] involve the determination of relative movements, the movements that occur between mobile reference systems:

$$x_0 = \omega_3^T(-\varphi_2) \cdot X_1 = x + A = \omega_3^T(\varphi_1) \cdot X + A \Leftrightarrow$$
$$\Leftrightarrow X_1 = \omega_3(-\varphi_2) \cdot \left[\omega_3^T(\varphi_1) \cdot X + A\right] \Leftrightarrow \qquad (5.4)$$
$$\Leftrightarrow X_1 = \omega_3^T(\varphi_2) \cdot \left[\omega_3^T(\varphi_1) \cdot X + A\right]$$

and the reverse movement:

$$X = \omega_3(\varphi_1) \cdot \left[\omega_3(\varphi_2) \cdot X_1 - A\right]. \qquad (5.5)$$

If the rolling condition is also taken into account, according to which the relative velocity in the gearing pole must be zero, meaning:

$$\varphi_1 \cdot R_1 = \varphi_2 \cdot R_2' \Rightarrow \frac{\varphi_1}{\varphi_2} = \frac{R_2'}{R_1} = 1, \qquad (5.6)$$

the following expressions are obtained for the relative velocities:

$$X_1 = \omega_3^T(\varphi) \cdot \left[\omega_3^T(\varphi) \cdot X + A\right]; \qquad (5.7)$$

$$X = \omega_3(\varphi) \cdot \left[\omega_3(\varphi) \cdot X - A\right], \qquad (5.8)$$

with $\varphi_1 = \varphi_2 = \varphi$.

The "virtual pole" method, developed in [45-50], involves identifying a point called the virtual pole, defined as the intersection between the normal to the Σ profile, taken through the current point on the profile, and the centrode conjugated to the profile, C_1 circle.

Subsequently, the value by which the *XY* system must be moved so that the virtual pole reaches the gearing pole is determined. In this way, the Willis theorem [2], [28-31], developed in Chapters 1 and 3, is respected. Therefore, in this position of the mobile system *XY*, the current point *M* is in contact with the corresponding point *M* on the profile of the driver screw.

In order to determine the virtual pole, it is start from the equations (5.1). The position vector of the current point *M* is, Figure 5.17:

$$\vec{r} = \left[2 \cdot R \cdot \sin u - a \cdot \sin(2 \cdot u)\right] \cdot \vec{i} + \left[2 \cdot R \cdot \cos u - a \cdot \cos(2 \cdot u)\right] \cdot \vec{j}. \qquad (5.9)$$
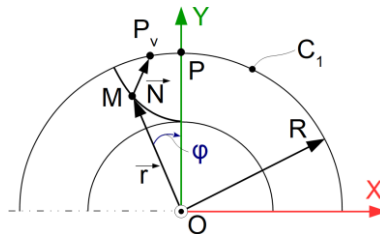
Fig. 5.17. The position vector of the current point *M*

The normal at this profile, taken from *M*, to the intersection with the C_1 centrode, has the equation:

$$\vec{N} = \lambda \cdot \left(\dot{Y}_u \cdot \vec{i} - \dot{X}_u \cdot \vec{j}\right) = \lambda \cdot \left[-2 \cdot R \cdot \sin u + 2 \cdot a \cdot \sin(2 \cdot u)\right] \cdot \vec{i} -$$
$$-\lambda \cdot \left[2 \cdot R \cdot \cos u - 2 \cdot a \cdot \cos(2 \cdot u)\right] \cdot \vec{j}, \qquad (5.10)$$

where λ represents the modulus of the vector $\vec{N}$.

Implementation of the „virtual pole" method for the study of the enwrapping surfaces determined by reverse engineering techniques

The position vector of the virtual pole, as a point belonging to the circle C_1 of radius R, is given by:

$$\vec{r_{P_v}} = (R \cdot sin\varphi) \cdot \vec{i} + (R \cdot cos\varphi) \cdot \vec{j}. \tag{5.11}$$

There is a relationship between vectors (5.9), (5.10) and (5.11):

$$\vec{N} + \vec{r} = \vec{r_{P_v}}, \tag{5.12}$$

relation that allows the elimination of the parameter λ:

$$\begin{aligned}
&\left[2 \cdot R \cdot sin\,u - a \cdot sin(2 \cdot u) + \lambda \cdot (-2 \cdot R \cdot sin\,u + 2 \cdot a \cdot sin(2 \cdot u)) \right] \cdot \vec{i} + \\
&+ \left[2 \cdot R \cdot cos\,u - a \cdot cos(2 \cdot u) - \lambda \cdot (2 \cdot R \cdot cos\,u - 2 \cdot a \cdot cos(2 \cdot u)) \right] \cdot \vec{j} = \\
&= (R \cdot sin\varphi) \cdot \vec{i} + (R \cdot cos\varphi) \cdot \vec{j}
\end{aligned} \tag{5.13}$$

Taking the relation (5.13), the enwrapping condition is obtained, meaning the φ value with which the *XY* system must be rotated so that the P_v point, corresponding to a certain value of the parameter *u*, overlaps the gearing pole:

$$\varphi = u + 2 \cdot arctg\left(\frac{R - a \cdot cos\,u}{a \cdot sin\,u} \right). \tag{5.14}$$

The identification of the point on the profile of the driver screw, which is in contact with the current point on the profile of the driven screw, is done by applying the movements (5.3).

Considering the coordinates of the current point *M* as:

$$M: \begin{vmatrix} X = X_M; \\ Y = Y_M, \end{vmatrix} \tag{5.15}$$

and these being known for a value of the *u* parameter, when rotating the *XY* system with the φ angle, given by the relation (5.14), in the fixed reference system, the point *M* will have the coordinates, according to equation (5.3):

$$x = \omega_3^T(\varphi) \cdot X$$

$$\begin{pmatrix} x \\ y \end{pmatrix} = \begin{pmatrix} cos\varphi & -sin\varphi \\ sin\varphi & cos\varphi \end{pmatrix} \cdot \begin{pmatrix} X_M \\ Y_M \end{pmatrix} = \begin{pmatrix} X_M \cdot cos\varphi - Y_M \cdot sin\varphi \\ X_M \cdot sin\varphi + Y_M \cdot cos\varphi \end{pmatrix} \Rightarrow \tag{5.16}$$

$$\Rightarrow M_x: \begin{vmatrix} x_M = X_M \cdot cos\varphi - Y_M \cdot sin\varphi; \\ y_M = X_M \cdot sin\varphi + Y_M \cdot cos\varphi. \end{vmatrix}$$

At this point, point *M* is on the contact curve. In the fixed reference system, x_0y_0, the same point has the coordinates given by the equation (5.2):

$$M_{x_0}: \begin{vmatrix} x_{0_M} = x_M; \\ y_{0_M} = y_M - 2 \cdot R. \end{vmatrix} \tag{5.17}$$

Considering (5.3), the coordinates of M_1 point, the contact point with *M*, are determined:

$$X_1 = \omega_3^T(\varphi) \cdot x_0;$$

$$M_1: \begin{vmatrix} X_{1_{M_1}} = x_{0_M} \cdot cos\varphi - y_{0_M} \cdot sin\varphi; \\ Y_{1_{M_1}} = x_{0_M} \cdot sin\varphi + y_{0_M} \cdot cos\varphi. \end{vmatrix} \tag{5.18}$$

In this way, when the u parameter varies so that the current point completely traverses the flank of the driven screw, the coordinates of the corresponding points on the profile of the diver screw can be identified.

Applying the described algorithm, the driver and the driven screws were modeled, Figures 5.18 and 5.19, and the numerical models obtained were compared with the scanned models.

Fig. 5.18. Virtual model of the driven screw　　　　Fig. 5.19. Virtual model of the driver screw

In order to compare the scanned model and the CAD model of the screws, from the *File -> Import* menu, the scanned model and the CAD model of the pieces are imported, the two models having different orientations in relation to the reference system prescribed in the program. The *Prealignment* command is used to overlap the two models into a single reference system and is compared by accessing the Surface Comparison on CAD command.

Finally, labels are created that show the numerical values of these deviations, using the *Deviation Label* command. The results are shown in Figures 5.20 and 5.21.

Fig. 5.20 Dimensional deviations in the case of the driven screw　　　　Fig. 5.21. Dimensional deviations in the case of the driver screw

Implementation of the „virtual pole" method for the study of the enwrapping surfaces determined by reverse engineering techniques

5.4. Inspection of worm shafts from the construction of worm gears-worm wheel

5.4.1. Graphical modelling of worm shafts in the construction of the seats adjustment mechanism of Audi and Mercedes cars

The graphical modeling of the worm shafts was made in *CATIA V5R21* program, a software package that makes the 3D modeling of solids as efficient and precise as possible, in the *Generative Shape Design* module. Graphical modeling of the worm shaft from the construction of the seat adjustment mechanism of an Audi car was made according to the dimensions in Figure 5.22, and the modeling of the worm shaft from the construction of the seat adjustment mechanism of a Mercedes car, according to the dimensions in Figure 5.23.
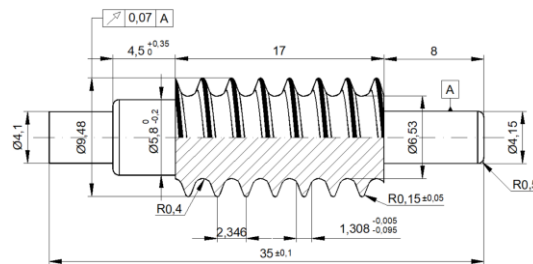
Fig. 5.22. The dimensions of the worm shaft from the construction of the seat adjustment mechanism of an Audi car
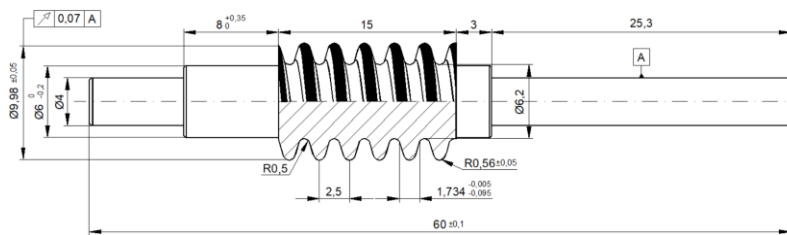
Fig. 5.23. The dimensions of the worm shaft from the construction of the seat adjustment mechanism of a Mercedes car

Therefore, following the modeling steps detailed in the doctoral thesis, Figures 5.24 and 5.25 show the numerical models of the worm shafts in the construction of the seat adjustment mechanism of Audi and Mercedes cars made in CATIA software.
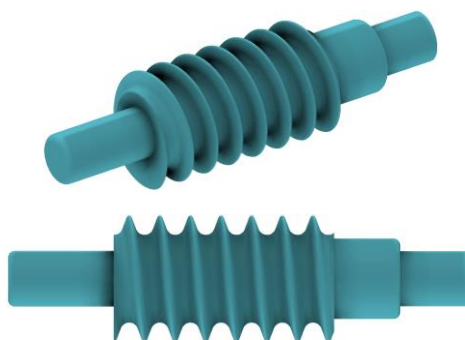
Fig. 5.24. Virtual model of the worm shaft from the construction of the seat adjustment mechanism of an Audi car
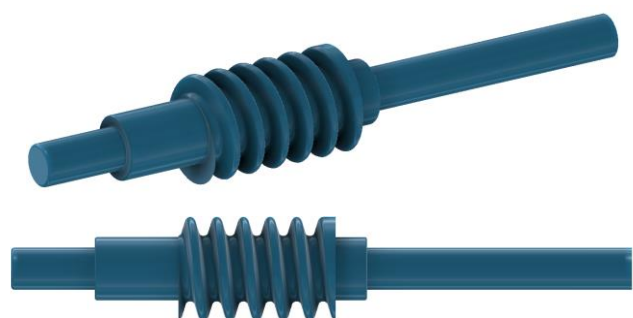
Fig. 5.25. Virtual model of the worm shaft from the construction of the seat adjustment mechanism of a Mercedes car

The modeled parts will be saved in **.stp* format, thus allowing them to be opened in the inspection program, in order to compare the CAD model with the scanned model of each part.

5.4.2. Comparison between the scanned model and the CAD model of worm shafts in the construction of the seats adjustment mechanism of Audi and Mercedes cars

The comparison between the scanned models and the CAD models of the pieces is made in GOM Inspect program. To import the two models - the scanned model, in **.stl* format and the CAD model, in **.stp* format, the "*New Project*" module from the inspection program will be selected.

Elements obtained by scanning will have a green marker in front of the name and the nominal ones, obtained from CAD modeling, will have a blue marker. For inspection, the actual model of the pieces obtained by scanning must be aligned with the nominal one, obtained by CAD modeling. Various alignment methods can be used, but the most convenient and at the same time the default method is the prealignment method. This achieves automatic alignment, independent of the scanning position of the physical model.

After the alignment between the nominal and the real data, the pieces can be inspected, which means that the deviations between the two data sets can be determined.

The result of the inspection is presented in the form of a map of the deviations in which they are symbolized by the colors: blue - negative deviation; green - zero deviation; red - positive deviation. Areas where the deviation has not been calculated are shown on the deviation map in gray. After creating the map, the program displays a legend of it. This legend represents the values corresponding to individual colors. Labels can be created on any color of the deviation representation to show the numerical values of these deviations, but in order to do so, the deviation map must first be represented.

Thus, the comparison of the two worm shafts is made using the *Surface Comparison on CAD* 🔧 command from *Inspection -> CAD Comparison* menu. The inspection which analyzes the imperfections of the worm shafts from the construction of the seat adjustment mechanism of Audi and Mercedes cars, depending on the two models, is done through the map of deviations, finally, creating labels that show the numerical values of these deviations, accessing the *Inspection -> Deviation Label* 🏷️ module, Figures 5.26 and 5.27.
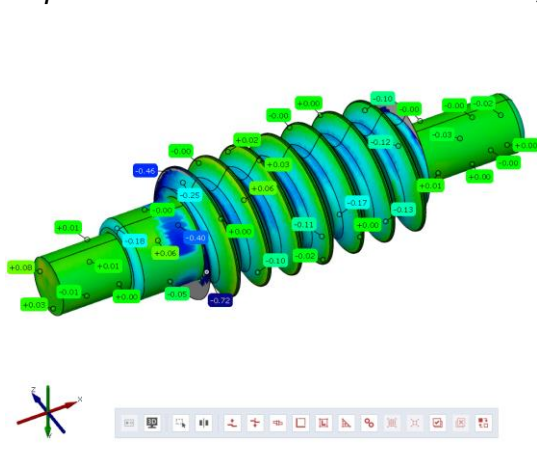
Fig. 5.26. Deviations in the case of the worm shaft from the construction of the seat adjustment mechanism of an Audi car
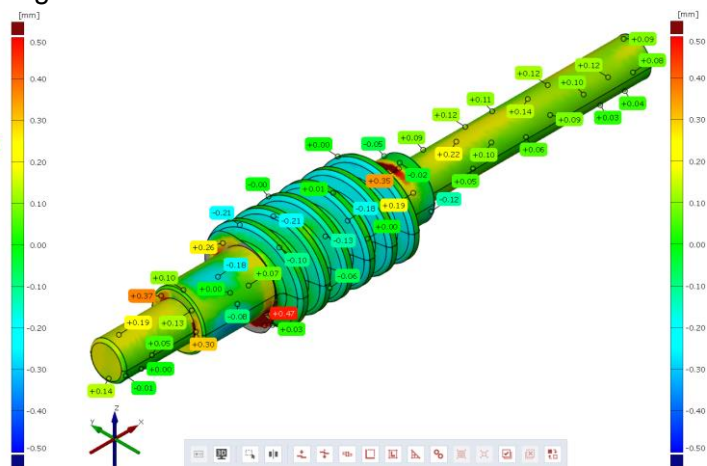
Fig. 5.27. Deviations in the case of the worm shaft from the construction of the seat adjustment mechanism of a Mercedes car

Eng. Georgiana Alexandra COSTIN (MOROȘANU) **Chapter 5**

Implementation of the „virtual pole" method for the study of the enwrapping surfaces determined by reverse engineering techniques

5.5. Conclusions regarding the implementation of the „virtual pole" method for the study of the enwrapping surfaces determined by reverse engineering techniques

In this chapter, a three-dimensional scanning technique applied to pieces with a complex geometry was presented, highlighting multiple advantages compared to the traditional CAD design, such as: speed in work, compared to CAD design; reduced time in transposing 3D pieces or digital models; higher speed in pieces inspection and control; precise determination of deviations compared to the initial geometric model etc.

The comparison of the scanned model with the CAD model obtained based on the measured dimensions demonstrates the quality of the designed model and the fact that it can be used as a basis for the realization of the execution documentation of the respective pieces.

Areas where there are significant deviations from the physical pattern are limited in extent and are exceptions. The appearance of these areas is explained by the imperfections of the pieces inspected by scanning and by the measurement difficulties caused by their complex shape and do not represent errors of the numerical models obtained by design.

Another source of error is the stage of preparing the pieces for scanning, namely covering them with a matte layer to prevent scanning defects caused by glossy surfaces.

CHAPTER 6. GENERAL CONCLUSIONS, PERSONAL CONTRIBUTIONS AND PERSPECTIVES

6.1. General conclusions

In this doctoral thesis, in the first stage, in Chapter 1, "State of the art regarding study methods for reciprocally enveloping surfaces", different methods of profiling the tools that generate by enwrapping, as well as methods of profiling tools for processing helical surfaces by the kinematic method, respectively by the method of decomposing the helical movement was presented, these being the results of some researchers in the field.

Analyzing all these methods, it was noticed that the profiling of the tools that generate by enwrapping requires the writing of relatively complicated computational equations, being sources of major errors. Thus, as an alternative to this problem, in this doctoral thesis was proposed a solution that can avoid these computational errors by developing a new complementary method, called the "virtual pole" method.

This method is based on a reinterpretation of the Willis theorem (normals theorem), which allows the analytical profiling of the tools that generate by enwrapping, by the rolling method, avoiding the need to write the equations of relative tool-part movements.

In order to respect the Willis theorem, when the normal to the generated profile must pass through a gearing pole, this being a tangency point between two conjugate centrodes (the centrode of the tool and that of the piece), that normal is common both for the profile to be generated and for the generating profile.

In order to highlight more clearly the advantage of the "virtual pole" method over the other specific methods of profiling the tools that generate by enwrapping by the rolling method, in Chapter 3, entitled "*Development of a tool profiling algorithm that generates by enwrapping - „virtual pole" method*, I presented a comparison between the "virtual pole" method and the Gohman theorem, customized for profiling a rack-type tool, designed to generate a shaft-type piece with square section.

In this way, it has been shown that the "virtual pole" method removes much of the calculations needed for profiling different types of tools, given that determining the relative movements between the tool and the piece as well as determining the enwrapping condition are relatively complicated and can be a source of major errors.

At the same time, in Chapter 3, I presented, in more detail, this complementary method, applied for profiling rack-type tool (for a shaft-type piece with square section and for generating an involute flank), gear shaped cutter tool (for generating a *K*-type bore) and rotary cutter tool (for processing a ball screw), which showed that the relative movements between the tool and the piece, in the case of the respective tools, were no longer necessary.

For these types of tools we imagined the algorithm for applying the method and developed a calculation program to allow the numerical determination of the sought profiles, noting that the numerical results are identical to those obtained using established methods of profiling tools that generates by enwrapping by the rolling method, such as the Gohman theorem or the normals theorem.

Numerical applications were made in the *Octave* program, being a software product designed for performing numerical calculations, especially for solving systems of equations that have linear algebra operations on vectors and matrices, being a program perfectly adapted to the needs of a technical application.

However, it should be noted that during the profiling process, the "virtual pole" method does not eliminate the influence of relative movements, but only the need to write these movements explicitly, meaning the need to work with relatively complex equations.

At the same time, the "virtual pole" theorem cannot be applied as such to disk type tools and cylindrical-front tools, due to the fact that this method is intended for the study of planar gearing.

However, the method can be used to identify the intermediate surface and, with the help of graphic design media, can provide a support for profiling the types of tools mentioned (disk tools, cylindrical-front tools, worm tools).

Examples of application of the "virtual pole" method in the case of worm tools, I presented in Chapter 4, entitled "*Profiling of worm tools for generating surfaces known in analytical or discrete form, by the „virtual pole" method*", in which we performed both profiling the worm toll intended for generating of the active surface of the cam of a cycloidal reducer, as well as the profiling of the worm tool generating an ordered curl, known in discrete form.

In the case of profiling worm tool intended to generate the active surface of the cam of a cycloidal reducer, the algorithm was based on determining an intermediate surface, belonging to the generating rack, which is reciprocally enveloping the surface of the cycloidal disk, the profiling algorithm using the advantages of the "virtual pole" method. Thus, the analytical equations of the cycloidal profile were known and we performed the profiling of the worm tool.

The intermediate surface was approximated by a family of plane stripe type surfaces, which were determined by approximating the generating curve with point cloud known in discrete form.

In the case of profiling the worm tool generating an ordered curl, known in discrete form, the discrete profile represented the profile of the active disk in the composition of a cycloidal reducer. The coordinates of some points on this profile was determined of by scanning.

At the same time, in the *Octave* and *CATIA* programs, we developed numerical applications for the profiling of the worm tool for processing the active surface of the cam of a cycloidal reducer and, respectively, for generating a profile known in discrete form, concluding that the calculation time for profiling is significantly reduced and the disadvantage of the resulting error is small enough to be technically acceptable and is fully compensated by this reduction of computation time, the error resulting from the fact that the intermediate surface was replaced with an approximate surface by strips (the normal being a curve and it was approximated by a straight line segment).

After applying the "virtual pole" method to the mentioned generating processes, we conducted a study on the inspection of reciprocally enveloping surfaces, using a three-dimensional measurement technique, namely reverse engineering, which involves 3D scanning of a component or subassembly.

This measurement technique was developed in Chapter 5, entitled "*Implementation of the „virtual pole" method for the study of the enwrapping surfaces determined by reverse engineering techniques*", from this doctoral thesis.

In this chapter, the 3D scanning of four pieces with helical surfaces was proposed and performed, namely two pieces of a helical pump (driver screw and driven screw) and two worm shafts from the construction of the seat adjustment mechanism of Audi and Mercedes cars.

The pieces were scanned with the help of Atos Core equipment, produced by the German company GOM, existing in the Department of Manufacturing Engineering, within the Faculty of Engineering, "Dunărea de Jos" University of Galați, with the help of the GOM Scan software.

The equipment was purchased in 2019 by the project "*Smart Manufacturing Technologies for Advanced Production of Parts From Automotive And Aeronautics Industries - TFI PMAIAA*", PN-III-P1-1.2-PCCDI-2017-0446 [64], the system based on a 3D optical scanner without physical contact.

The scanning process of the four types of pieces consisted of: applying the reference markers, both on the pieces and on the table of the scanning equipment, so that they can be recognized by the equipment and the *GOM Scan* software; applying an anti-reflective spray to the pieces so that the glossy surfaces of the parts to become matte surfaces (due to the fact that glossy surfaces generally lead to low scanning quality); the actual scanning process of the pieces in which several scans from different angles were necessary, in order to completely digitize the objects; the polygonalization process, which represents the correlation of all the scans of each piece and the obtaining of complete numerical models.

After completing the scanning process, the active elements of the helical pump, namely the driver screw and the driven screw, were measured by means of a specific software called *GOM Inspect*, in order to establish their dimensional characteristics and their modeling in a dedicated software program, called *CATIA V5R21*, a software package which makes 3D modeling of solids as concrete and precise as possible.

At the same time, we realized a study of the enwrapping of the active surfaces of the helical pump elements by analyzing the frontal profiles, using the "virtual pole" method.

Thus, starting from the front profile of the driven screw, the reciprocally enwrapping profile corresponding to the driver screw was determined and based on this profile, the driven screw was modeled, the numerical model obtained being later compared to the model obtained by scanning, by GOM Inspect software.

After scanning the worm shafts from the gears, more precisely from the construction of the seat adjustment mechanisms of Audi and Mercedes cars, the obtained models were compared with the numerical models based on the execution drawings, in order to estimate the dimensional deviations of the pieces.

Although the four types of scanned pieces had a complex geometry, three-dimensional scanning offered multiple advantages over CAD design, advantages such as: speed in work; reduced time to transpose 3D parts; precise determination of dimensional deviations compared to the initial geometric model etc.

The comparison between the scanned pieces and the CAD models, obtained on the basis of the measured dimensions, demonstrated the quality of the designed models and the fact that they can be used as a basis for the realization of the execution documentation of those pieces. Areas where significant dimensional deviations from physical pieces occur are limited in extent and are exceptions.

The appearance of these areas is explained by the imperfections of the pieces inspected by scanning and by the measurement difficulties caused by their complex form and do not represent errors of the numerical models obtained by design.

Another source of error is the preparation steps of the pieces for the scanning process, respectively covering them with a matte layer, using an anti-reflective spray, which would prevent the scanning defects caused by the glossy surfaces. If the coverage is not uniform, errors may occur in the form of gaps in the point cloud. At the same time, if the layer thickness is too large, dimensional shape deviations may occur, which may be outside the permissible tolerance limits [65].

At the same time, during the scanning process, the Atos Core equipment allows the choice of different exposure times, so that a complete picture of the scanned surfaces can be obtained, even in the conditions where there are areas with relatively important color differences [65].

If the exposure times are not properly selected in terms of number or duration (it is recommended that the number of exposure times be kept to a minimum, as each additional exposure time increases the scan time), areas that may be overexposed or underexposed will appear, manifesting as gaps in the resulting point cloud [65].

6.2. Personal contributions

The personal contributions from this doctoral thesis represented:

- the preparation of the documentation, in order to prepare the state of the art regarding the different tool profiling methods that generate by enwrapping by the rolling method, as well as tool profiling methods for processing helical surfaces by kinematic method, respectively by the method of helical decomposition;

- development of the "virtual pole" method, as well as the algorithms for profiling the tools such as rack, gear shaped cutter, rotary cutter and worm tool, using this method;

- realization of numerical applications in the Octave program for: profiling of rack-type tools, for a shaft-type piece with square section and for generating an involute flank; profiling of gear shaped cutte tools, for generating a *K*-type bore; profiling of rotary cutter tools for processing a ball screw; for profiling worm-type tools for processing the active surface of the cam of a cycloidal reducer and for generating a profile known in discrete form (the cycloidal disk of a cycloidal reducer);

- obtaining the profiles and identifying the surfaces by scanning the cycloidal disk, the two pieces of a helical pump (the driver screw and the driven screw) and the two worm shafts from the construction of the seat adjustment mechanisms of Audi and Mercedes cars, as well as the inspection of the surfaces of the scanned pieces (in the case of the pieces of the helical pump), in order to establish their dimensional characteristics;

- graphical modeling of the driver screw, the driven screw, as well as the two worm shafts from the construction of the seat adjustment mechanisms of Audi and Mercedes cars, in order to compare the scanned models with the CAD models, for the establishment of their dimensional deviations;

- definition of algorithms for inspection of pieces with helical active surfaces;

- realization of the study of the enwrapping of the helical surfaces, by analyzing the frontal profiles, using the "virtual pole" method, for the driver screw and the driven screw.

6.3. Perspectives

Following the study realized in this doctoral thesis, several future research directions can be considered:

- application of the "virtual pole" method for the corrective profiling of tools that generate by enwrapping, by the rolling method; a first paper was published regarding the corrective profiling of a gear shaped cutter tool (IMANEE 2021);

- extension of study methods for enwrapping helical surfaces by analyzing frontal profiles using the "virtual pole" method;

- conception of a profiling algorithm based on which an application will be made in a high-level programming language, which allows the profiling of the aforementioned tools (implementation of VBA application (*Visual Basic for Applications*) made in the CATIA software program).

- publishing a chapter in a book published by a prestigious international publishing house (Springer), in which will be presented an application integrated in a graphic design environment (CATIA), the application being intended for profiling the tools that generate by rolling, based on the "virtual pole" method.

List of published scientific articles

A. Scientific articles published in journals indexed by Thomson Reuters - Web of Science (ISI), with Impact Factor

1. N. Baroiu, **G. A. Costin,** V. G. Teodor, D. Nedelcu, V. Tăbăcaru, *Prediction of Surface Roughness in Drilling of Polymers using a Geometrical Model and Artificial Neural Networks*, revista Materiale Plastice, Vol. 57, Issue 3, ISSN 2668-8220 (Online), 0025-5289 (Print), pp 160-173, Impact factor 2020 - 0.593, 2020, https://revmaterialeplastice.ro/Articles.asp?ID=5390.

B. Scientific articles published in journals and volumes of conferences indexed by Thomson Reuters - Web of Science (ISI)

1. **G. A. Moroşanu,** N. Baroiu, V. G. Teodor, V. Păunoiu, N. Oancea, *Review on Study Methods for Reciprocally Enwrapping Surfaces, Inventions*, Vol. 7, Issue 1, pp. 1-33, 2022, ISSN 2411-5134, https://www.mdpi.com/2411-5134/7/1/10;

2. N. Baroiu, **G. A. Moroşanu,** V. G. Teodor, N. Oancea, *Roller Profiling for Generating the Screw of a Pump with Progressive Cavities*, Inventions Journal, Vol. 6, Issue 2, pp. 1-8, ISSN 2411-5134, 2021, https://www.mdpi.com/2411-5134/6/2/34 **(single corresponding author)**;

3. **G. A. Costin**, V. G. Teodor, N. Oancea „*Virtual Pole*" *method applied at the profiling of the rotary cutter tool for processing of ball screw*, ModTech International Conference Modern Technologies in Industrial Engineering, IOP Conf. Series: Materials Science and Engineering, Vol. 916, ISSN 1757-899X (Online), 1757-8981 (Print), 2020, https://iopscience.iop.org/article/10.1088/1757-899X/916/1/012022.

4. V. Păunoiu, V. G. Teodor, C. Afteni, **G. A. Costin**, N. Baroiu, *Application of 3D scanning in inspection of the automotive body parts,* The XXXI-st SIAR International Automotive and Transport Engineering Congress, 28.10-30.10.2021, Chișinău, Republica Moldova, Revista Ingineria automobilului, Nr. 62, pp. 9-13, ISSN 1842 - 4074, 2022, http://siar.ro/publicatii/; http://siar.ro/wp-content/uploads/2022/04/rIA-62-1.pdf;

C. Scientific papers published in journals indexed by international databases (IDB)

1. **G. A. Moroşanu**, V. G. Teodor, R. S. Crăciun, *Corrective profiling method for tools that generate by enwrapping*, The 25th Edition of Innovative Manufacturing Engineering & Energy International Conference (IMANEE), 21-23 October 2021 (online edition), IOP Conference Series: Materials Science and Engineering, Vol. 1235, 012020, doi:10.1088/1757-899X/1235/1/012020, ISSN 1757-899X (Online), 1757-8981 (Print), 2022, https://iopscience.iop.org/article/10.1088/1757-899X/1235/1/012020/meta;

2. **G. A. Moroşanu,** V. Păunoiu, V. G. Teodor, N. Baroiu, *Design and graphic modeling of fixturing devices specialized for manufacturing industry*, Journal of Industrial Design and Engineering Graphics - JIDEG, Vol 16, No 1, pp. 21-26, ISSN 1843-3766, 2021, http://sorging.ro/jideg/index.php/jideg/article/view/245;

3. **G. A. Moroşanu,** V. G. Teodor, N. Oancea, *Profiling of the generating rack of an ordered curl known in discrete form by the virtual pole method*, Buletinul Institutului Politehnic din Iaşi (Bulletin of the Polytechnic Institute of Iaşi), Vol. 67 (71), No. 4, pp. 25-34, 2021, https://www.cmmi.tuiasi.ro/wp-content/uploads/buletin/2021%20fasc%204/L3_CMMI%204_2021.pdf;

4. N. Baroiu, **G. A. Moroşanu,** S. S. Chislitschi, *Self-Cleaning System Filter Treating Installation of the Ballast Water for Ships*, TEHNOMUS Journal - New Technologies and Products in Machine Manufacturing Technologies, No. 28, ISSN-1224-029X, pp. 9-18, 2021, http://www.fim-old.usv.ro/conf_1/tehnomusjournal/pagini/journal2021/files/01.pdf;

5. **G. A. Moroşanu**, N. Baroiu, *Study on Small and Medium-Sized Boats with Ecological Propulsion Systems in Danube Delta Area*, Journal of Danubian Studies and Research, Vol. 11, No. 1, 2021, pp. 172-183, ISSN: 2284-5224, https://dj.univ-danubius.ro/index.php/JDSR/article/view/1291;

6. N. Baroiu, P. Chebac, **G. A. Moroşanu**, *Control and Management of Ballast Water on Commercial Ships*, Journal of Danubian Studies and Research, Vol. 11, No.1, 2021, pp. 160-171, ISSN: 2284-5224, https://dj.univ-danubius.ro/index.php/JDSR/article/view/1292;

7. **G. A. Moroşanu**, V. G. Teodor, N. Baroiu, *Aspects Regarding the Organization and Functioning of the Student Entrepreneurial Societies (SES) in Higher Education System from Romania*, EIRP

Proceedings, Vol. 16, No. 1, pp. 386-395, ISSN 2067 - 9211 (Print), 2069 – 9344 (Online), 2021, https://dp.univ-danubius.ro/index.php/EIRP/article/view/192;

8. N. Baroiu, **G. A. Costin**, G. R. Frumușanu, V. G. Teodor, N. Oancea, *Study of the stator geometry for a Moineau pump*, The 5th International Conference on Computing and Solutions in Manufacturing Engineering - COSME 2020, IOP Conference Series: Materials Science and Engineering, 1009, 012003, doi:10.1088/1757-899X/1009/1/012003, ISSN 1757-899X (Online), 1757-8981 (Print), 2021, https://iopscience.iop.org/article/10.1088/1757-899X/1009/1/012003/pdf **(single corresponding author)**;

9. N. Baroiu, **G. A. Moroșanu**, *Graphical Modelling and Studies on Hydraulic Pump Parameters*, Journal of Industrial Design And Engineering Graphics - JIDEG, Vol. 15, No. 2, Issue 2, pp. 7-12, ISSN 2344-4681 (Online), 1843-3766 (Print), 2020, http://sorging.ro/jideg/index.php/jideg/article/view/127;

10. **G. A. Costin,** V. G. Teodor, N. Baroiu, V. Păunoiu, *Graphical modelling of a hydromechanical drawing die*, Journal of Industrial Design And Engineering Graphics - JIDEG, Vol. 15, No. 2, Issue 2, pp. 21-26, ISSN 2344-4681 (Online), 1843-3766 (Print), 2020, http://sorging.ro/jideg/index.php/jideg/article/view/130;

11. **G. A. Costin,** N. Baroiu, V. G. Teodor, V. Păunoiu, N. Oancea, *Tool's Profiling for Rotational Volumetric Deformation - Analytical Study,* 6th International Conference on Advanced Manufacturing Engineering and Technologies - NEWTECH 2020, IOP Conference Series: Materials Science and Engineering, Vol. 968, 2020, https://iopscience.iop.org/article/10.1088/1757-899X/968/1/012016/meta;

12. N. Baroiu, **G. A. Costin,** V. G. Teodor, N. Oancea, *Algorithm for screws profiling of a conical trilobed compressor - analytical solution*, 6th International Conference on Advanced Manufacturing Engineering and Technologies - NEWTECH 2020, IOP Conference Series: Materials Science and Engineering, Vol. 968, 2020 **(single corresponding author)**, https://iopscience.iop.org/article/10.1088/1757-899X/968/1/012030;

13. **G. A. Costin**, V. G. Teodor, *Virtual pole method applied at the profiling of the gear shaped cutter tool for generating a K-type bore*, 7th International Conference on Manufacturing and Materials Engineering - ICMMEN, MATEC Web of Conferences, Vol. 318, ISSN 2261-236X, 2020, https://doi.org/10.1051/matecconf/202031801001;

D. Other publications

1. **G. A. Moroşanu,** V. G. Teodor, N. Oancea, *Gear-rack tool for generating an involute flank. Virtual pole method*, The Annals of "Dunărea de Jos" University of Galati, Fascicle V, pp. 25-28, ISSN 1221-4566, 2021, http://www.cmrs.ugal.ro/TMB/2021/L04_Morosanu_G.pdf;

2. M. Oprea, **G. A. Moroşanu,** V. G. Teodor, V. Păunoiu, *Verification through three-dimensional scanning of a part made by rapid prototyping technologies*, The Annals of "Dunărea de Jos" University of Galati, Fascicle V, pp. 35-40, ISSN 1221-4566, 2021, http://www.cmrs.ugal.ro/TMB/2021/L06_Oprea_M.pdf;

3. R. S. Crăciun, **G. A. Moroşanu,** V. G. Teodor, *Improving the quality of small pieces made by rapid prototyping*, The Annals of "Dunărea de Jos" University of Galati, Fascicle V, pp. 19-24, ISSN 1221-4566, 2021, http://www.cmrs.ugal.ro/TMB/2021/L03_Craciun_R.pdf;

4. **G. A. Moroşanu,** R. S. Crăciun, N. Baroiu, *Constructive-functional analysis and calculation of flow control valves*, The Annals of "Dunărea de Jos" University of Galati, Fascicle V, pp. 29-34, ISSN 1221-4566, 2021, http://www.cmrs.ugal.ro/TMB/2021/L05_Morosanu_G.pdf;

5. N. Baroiu, **G. A. Moroşanu**, *Constructive-functional analysis and sizing of hydraulic filters*, The Annals of "Dunărea de Jos" University of Galati, Fascicle V, pp. 5-10, ISSN 1221-4566, 2021, http://www.cmrs.ugal.ro/TMB/2021/L01_Baroiu_N.pdf;

6. V. G. Teodor, **G. A. Costin**, *Virtual Pole Method - Alternative Method for Profiling Rack Tools*, The Annals of „Dunărea de Jos" University of Galati, Fascicle V, pp. 5-8, ISSN 2668-4888 (Online), 2668-4829 (Print), 2019, http://www.cmrs.ugal.ro/TMB/2019/L_01_Teodor.pdf;

7. **G. A. Costin**, V. G. Teodor, N. Oancea, *The Virtual Pole Method - An Alternative Method for Profiling Tools which Generate by Enwrapping*, The Annals of „Dunărea de Jos" University of Galati, Fascicle V, pp. 31-34, ISSN 2668-4888 (Online), 2019, http://www.cmrs.ugal.ro/TMB/2019/L_05_Costin.pdf;

8. I. Iacob, **G. A. Costin**, C. Afteni, V. Păunoiu, *Modeling of Sheet Metal Forming using Quasi-Elastic Media*, The Annals of „Dunărea de Jos" University of Galati, Fascicle V, pp. 35-38, ISSN 2668-4888 (Online), 2668-4829 (Print), 2019, http://www.cmrs.ugal.ro/TMB/2019/L_06_Iacob.pdf.

REFERENCES

[1] Radzevich S. P., *Kinematic Geometry of Surface Machining*, CRC Press: London, UK, 2008;

[2] Oancea N., *Surfaces Generation through Winding, Vol. I-III*, Galați University Press: Galați, Romania, 2004;

[3] Chan C. L., Ting K. L. Extended Camus Theory and Higher Order Conjugated Curves, *Journal of Mechanisms and Robotics*, Vol. 11, pp. 1-9, 2019;

[4] Teodor V. G. *Contributions to the Elaboration of a Method for Profiling Tools. Tools which Generate by Enwrapping*, Lambert Academic Publishing: Saarbrücken, Germany, 2010;

[5] Dana-Picard T., Zehavi N., *Automated study of envelopes of one-parameter families of surfaces*, Springer Proceedings in Mathematics & Statistics, Vol. 198, pp. 29-44, 2017;

[6] Dooner D. B., *On the Third Law of Gearing: A Study on Hypoid Gear Tooth Contact*, Mechanism and Machine Theory, Vol, 134, pp. 224-248, 2019;

[7] Albu S. C., *Simulation of Processing of a Helical Surface with the Aid of a Frontal-Cylindrical Milling Tool*, Procedia Manufacturing, Vol. 32, pp. 36-41, 2019;

[8] Guo Q., Qing G. G., Jiang Y., *An Analytic Method of Computing the Envelope Surface of General Cutter with Runout in 5-axis Machining for Manufacturing Systems*, *Chinese Journal of Mechanical Engineering*, Vol. 38, pp. 403-412, 2017;

[9] Albu S. C., *Simulation of Processing of a Helical Surface with the Aid of a Frontal-Cylindrical Milling Tool*, Procedia Manufacturing, Vol. 32, pp. 36-41, 2019;

[10] Huai C., Zhao Y., *Meshing Theory and Tooth Profile Geometry of Toroidal Surface Enveloping Conical Worm Drive*, Mechanism and Machine Theory, Vol. 134, pp. 476-498. 2019;

[11] Jia K., Zheng S., Guo J., Hong J., *A Surface Enveloping-Assisted Approach on Cutting Edge Calculation and Machining Process Simulation for Skiving*, International Journal of Advanced Manufacturing Technology, Vol. 100, pp. 1635-1645, 2019;

[12] Liu Z., Lu H., Yu G., Wang S., *A Novel CNC Machining Method for Enveloping Surface,* International Journal of Advanced Manufacturing Technology, Vol. 85, pp. 779-790, 2016;

[13] Liu Z., Tang Q., Liu N., Song J., *A Profile Error Compensation Method in Precision Grinding of Screw Rotors*, International Journal of Advanced Manufacturing Technology, Vol. 100, pp. 2557-2567, 2019;

[14] Meng Q., Zhao Y., Yang Z., *Meshing Limit Line of the Conical Surface Enveloping Conical Worm Pair*, Proceedings of the Institution of Mechanical Engineers, Part C: Journal of Mechanical Engineering Science, Vol. 234, pp. 693-703, 2020;

[15] Meng Q., Zhao Y., Yang Z., Cui J., *Meshing Theory and Error Sensitivity of Mismatched Conical Surface Enveloping Conical Worm Pair*, Mechanism and Machine Theory, Vol. 145, pp. 1-33, 2020;

[16] Yang J., Li H., Rui C., Wei W., Dong X., *A Method to Generate the Spiral Flutes of an Hourglass Worm Gear Hob*, Journal of Mechanical Design, Vol. 140, pp. 1-12, 2018;

[17] Zhao Y., Kong X., *Meshing Principle of Conical Surface Enveloping Spiroid Drive*, Mechanism and Machine Theory, Vol. 123, pp. 1-26, 2018;

[18] Zhou Y., Wu Y., Wang L., Tang J., Ouyang H., *A new closed-form calculation of envelope surface for modeling face gears*, Mechanism and Machine Theory, Vol. 137, pp. 211-226, 2019;

[19] Berbinschi S., Teodor V. G., Baroiu N., Oancea N., *The Substitutive Circles Family Method -Graphical Aproach in CATIA Design Environment*, The Annals of ''Dunarea de Jos'' University of Galati, Fascicle V, Technologies in Machine Building, pp. 53-66, ISSN 1221- 4566, 2013;

[20] Baroiu N., Berbinschi S., Teodor V. G., Oancea N., *Comparative Study of Drill's Flank Geometry Developed with the CATIA Software*, The Annals of ''Dunarea de Jos'' University of Galati, Fascicle V, Technologies in Machine Building, pp. 27-32, ISSN 1221- 4566, 2012;

[21] Baroiu N., Berbinschi S., Teodor V. G., Susac F., Oancea N., *The Complementary Graphical Method used for Profiling Side Mill for Generation of Helical Surface*, IOP Conference Series: Materials Science and Engineering, Vol. 227, 2017, ModTech International Conference Modern Technologies in Industrial Engineering, Sibiu, Romania, 14-17 June 2017;

[22] Baroiu N., Baroiu L., Teodor V. G., Ciocan T. L., *Graphical Method for Profiling the Side Mill which Generate Helical Flute of Tungsten Carbide Dental Cross Cut Bur*, Romanian Journal of Materials*, Vol. 48, pp. 131-139, 2018;

[23] Berbinschi S., Teodor V. G., Oancea N, *3D Graphical Method for Profiling Gear Hob Tools*, International Journal of Advanced Manufacturing Technology, Vol. 64, pp. 291-304, 2013;

[24] Berbinschi S., Teodor V. G., Baroiu N., Oancea N., *Enwrapping Surfaces with Point Contact-Comparison between CATIA Method and Analytical One*, The Annals of "Dunarea de Jos" University of Galati, Fascicle V, Technologies in Machine Building, Vol. 2, pp. 117-122, ISSN 1221- 4566, 2011;

[25] Berbinschi S., Teodor V. G., Frumuşanu G. R., Oancea N., *Graphical Method for Profiling the Tools which Generate Internal Surfaces by Rolling*, Academic Journal of Manufacturing Engineering, Vol. 12, pp. 12-17, 2014;

[26] Berbinschi S., Teodor V. G., Oancea N., *A Graphical Method Developed in CATIA Design Environment for the Modeling of Generation by Enveloping*, The Annals of "Dunarea de Jos" University of Galati, Fascicle V, Technologies in Machine Building, Vol. 1, pp. 25-30, ISSN 1221- 4566, 2011;

[27] Berbinschi S., Baroiu N., Teodor V. G., Oancea N., *Profiling Method of Side Mill for Threading Screw for Dental Implants*, Advanced Materials Research Vol. 837, pp. 22-27, 2014;

[28] Moroşanu G. A., Baroiu N., Teodor V. G., Păunoiu V., Oancea N., *Review on Study Methods for Reciprocally Enwrapping Surfaces*, Inventions Journal, Vol. 7, Issue 1, pp. 1-33, ISSN 2411-5134, 2022;

[29] Oancea N., *Méthode numérique pour l'étude des surfaces enveloppées*, Mechanism and Machine Theory, Vol. 31, pp. 957-972, 1996;

[30] Carmo M. P., *Differential Geometry of Curves and Surfaces*, Courier Dover Publications: New York, USA, 2016;

[31] Dooner D. B., Griffis M. W., *On spatial Euler-Savary Equations for Envelopes*, ASME - Journal of Mechanical Design, Vol. 129, pp. 865-875, 2007;

[32] Berbinschi S., Teodor V. G., Oancea N., *A 3D Method for Profiling the Shaping Tool for the Generation of Helical Surfaces*, The Annals of "Dunarea de Jos" University of Galati, Fascicle V, Technologies in Machine Building, pp. 19-24, ISSN 1221- 4566, 2011;

[33] Teodor V. G., Baroiu N., Susac F., Oancea N., *The Modelling of Involute Teeth Generation with the Relative Generating Trajectories Method*, Academic Journal of Manufacturing Engineering - AJME, Vol. 14, pp. 126-131, 2016;

[34] Baroiu N., Teodor V. G., Popa C., Oancea N., *Gear Shaped Cutter - A Profiling Method Developed in Graphical Form*, The Annals of "Dunarea de Jos" University of Galati, Fascicle V, Technologies in Machine Building, pp. 9-16, ISSN 1221- 4566, 2015;

[35] Teodor V. G., Popa I., Oancea N., *The profiling of End Mill and Planing Tools to Generate Helical Surfaces Known by Sampled Points*, International Journal of Advanced Manufacturing Technology, Vol. 51, pp. 439-452, 2010;

[36] Baroiu N., Teodor V. G., Susac F., Oancea N., *Hob mill for trilobed rotor-Graphical method in CATIA*, IOP Conference Series: Material Science and Engineering, Vol. 448, pp. 1-17, 2018;

[37] Teodor V. G., Baroiu N., Berbinschi S., Susac F., Oancea N., *A Graphical Solution in CATIA for Profiling End Mill Tool which Generates a Helical Surface*, IOP Conference Series: Material Science and Engineering, Vol. 227, pp. 1-15, 2017;

[38] Baroiu N., Teodor V. G., Susac F., Oancea N., *Hob Mill Profiling Method for Generation of Timing Belt Pulley*, In Proceedings of the 5th International Conference on Advanced Manufacturing and Technologies (NewTech), Belgrade, Serbia, 6-9 June 2017, pp. 13-26;

[39] Berbinschi S., Teodor V. G., Baroiu N., Oancea N., *Profiling Methodology for Side Mill Tools for Generation of Helical Compressor Rotor using Reverse Engineering*, The Annals of "Dunarea de Jos" University of Galati, Fascicle V, Technologies in Machine Building, Vol. 2, pp. 111-116, ISSN 1221- 4566, 2011;

[40] Berbinschi S., Teodor V.G., Oancea N., *A study on helical surface generated by the primary peripheral surfaces of ring tool*, International Journal of Advanced Manufacturing Technology, Vol. 61, pp. 15-24, 2012;

[41] Berbinschi S., Teodor V. G., Oancea N., *3D Graphical Method fo Profiling Tools that Generate Helical Surfaces*, International Journal of Advanced Manufacturing Technology, Vol. 60, pp. 505-512, 2012;

[42] Berbinschi S., Teodor V. G., Oancea N., *Ring Tangential Tool Topological Representation of Peripheral Surfaces*, The Annals of "Dunarea de Jos" University of Galati, Fascicle V, Technologies in Machine Building, pp. 11-18, ISSN 1221- 4566, 2011;

[43] Frumuşanu G. R., Teodor V. G., Oancea N., *Graphical Method in CATIA to Profile the Hob Mill for Generating the Slitting Saw Cutter Teeth*, Applied Mechanics and Materials, Vol. 811, pp. 85-91, 2015;

[44] Teodor V. G., Baroiu N., Susac F., Oancea N., *Tangential Ring Tool - Graphical Profiling Method in CATIA*, 7th International Conference Manufacturing Technology - PILSEN, 2017, pp. 282-291;

[45] Costin G. A., Teodor V. G., Oancea N., *The Virtual Pole Method - An Alternative Method for Profiling Tools which Generate by Enwrapping*, The Annals of "Dunărea de Jos" University of Galati, Fascicle V, pp. 31-34, ISSN 2668-4888 (Online), 2668-4829 (Print), 2019;

[46] Teodor V. G., Costin G. A., *Virtual Pole Method - Alternative Method for Profiling Rack Tools,* The Annals of "Dunărea de Jos" University of Galati, Fascicle V, pp. 5-8, ISSN 2668-4888 (Online), 2668-4829 (Print), 2019;

[47] Moroşanu G. A., Teodor V. G., Oancea N., *Gear-rack tool for generating an involute flank. Virtual pole method*, The Annals of "Dunărea de Jos" University of Galati, Fascicle V, pp. 25-28, ISSN 1221-4566, 2021;

[48] Costin G. A., Teodor V. G., *Virtual pole method applied at the profiling of the gear shaped cutter tool for generating a K-type bore*, 7th International Conference on Manufacturing and Materials Engineering - ICMMEN, MATEC Web of Conferences, Vol. 318, ISSN 2261-236X, pp. 1-6, 2020;

[49] Costin G. A., Teodor V. G., Oancea N., *„Virtual Pole" method applied at the profiling of the rotary cutter tool for processing of ball screw*, ModTech International Conference Modern Technologies in Industrial Engineering, IOP Conf. Series: Materials Science and Engineering, Vol. 916, ISSN 1757-899X (Online), 1757-8981 (Print), pp. 1-6, 2020;

[50] Moroșanu G. A., Teodor V. G., Oancea N., *Profiling of the generating rack of an ordered curl known in discrete form by the virtual pole method*, Buletinul Institutului Politehnic din Iaşi (Bulletin of the Polytechnic Institute of Iaşi), Vol. 67 (71), Nr. 4, pp. 25-34, 2021;

[51] Litvin F. L., *Theory of Gearing,* Reference Publication 1212, NASA, Scientific and Technical Information Division: Washington, DC, USA, 1984;

[52] Teodor V. G., Baroiu N., Susac F., *The Synthesis of New Algorithms for CAD Profiling of Cutting Tools*, Lambert Academic Publishing: Saarbrücken, Germany, 2018;

[53] Susac F., Teodor V. G., Baroiu N., Oancea N., *Hob mill for spline shaft, profiled by generating trajectories method. Graphical application in CATIA*, MATEC Web of Conferences, Vol. 112, 2017;

[54] Teodor V. G., Berbinschi S., Baroiu N., Oancea N., *Graphical method for profiling hob mill that generate cycloid worms*, IOP Conference Series: Material Science and Engineering, Vol. 95, 2015;

[55] Teodor V. G., Baroiu N., Berbinschi S., Oancea N., *A Graphical Expression for the Method of Substitutive Circles Family Applied for Profiling Side Mill Designed to Generate Sealing Worms of Cycloid Pumps*, Applied Mechanics and Materials, Vols. 809-810, pp. 998-1003, 2015;

[56] Lai T. S., *Geometric design of roller drives with cylindrical meshing elements*, Mechanism and Machine Theory, Vol. 40, pp. 55-67, 2005;

[57] Peng Y., Song A., Shen Y., Lin X., *A novel arc-tooth-trace cycloid cylindrical gear*, Mechanism and Machine Theory, Vol. 118, pp. 180-193, 2017;

[58] Du J., Fang Z., *An active tooth surface design methodology for face-hobbed hypoid gears based on measuring coordinates*, Mechanism and Machine Theory, Vol. 99, pp. 140-154, 2016;

[59] *** Internet, *Spectromas, Sisteme optice marca GOM*, http://spectromas.ro/gama-atos-sisteme-de-scanare-3d-non-contact/, *Accesat: 10.04.2022*;

[60] *** Internet, *ATOS Core in use with GOM Scan software*, https://www.youtube.com/watch?v=751kz4SF7ME, Accesat: 12.04.2022;

[61] *** Internet, Universität Rostock, *3D-Scanner, ATOS 3D-Scanner + ARAMIS 3D-Kamera*, https://www.lfm.uni-rostock.de/ausstattung-informationen/analyse/3d-scanner/, Accesat: 13.04.2022;

[62] Yan D., Tang Q., Kovacevic A., Rane S, Pei L., *Rotor profile design and numerical analysis of 2–3 type multiphase twin-screw pumps*, Proceedings of the Institution of Mechanical Engineers, Part E: Journal of Process Mechanical Engineering, Vol. 232, Issue 2, pp. 186-202, 2017;

[63] Dong P., Zhao S., Zhao Y., Zhang P., Wang Y., *Design and experimental analysis of end face profile of tri-screw pump*, Proceedings of the Institution of Mechanical Engineers, Part A: Journal of Power and Energy, Vol. 234, Issue 4, pp. 481-489, 2019;

[64] *** Internet, *TFI PMAIAA*, http://www.tfipmaiaa.ugal.ro/obgen.html, Accesat: 18.04.2022;

[65] Afteni C., Păunoiu V., Afteni M., Teodor V.G., *Using 3D scanning in assessing the dimensional accuracy of mechanically machined parts*, The 25th Edition of IManEE 2021 International Conference, IOP Conference Series: Materials Science and Engineering, Vol. 1235, pp. 1-10, 2022.